RADC-TR-75-
Technical Report
June 6, 1975

NONLINEAR INTERACTION OF A NARROW SURFACE SPECTRUM WITH A PRESCRIBED SURFACE CURRENT

Physical Dynamics, Inc.

Sponsored By
Defense Advanced Research Projects Agency
ARPA Order No. 1649

Approved for public release;
distribution unlimited.

The views and conclusions contained in this document are those of the authors and should not be interpreted as necessarily representing the official policies, either expressed or implied, of the Defense Advanced Research Projects Agency or the U. S. Government.

Rome Air Development Center
Air Force Systems Command
Griffiss Air Force Base, New York

If this copy is not needed, return to RADC (OCSE/ Richard Carman) GAFB NY 13441.

NONLINEAR INTERACTION OF A NARROW SURFACE SPECTRUM WITH A PRESCRIBED SURFACE CURRENT

Bruce J. West
Bruce I. Cohen
Kenneth M. Watson

Contractor: Physical Dynamics, Inc.
Contract Number: F30602-72-C-0494
Effective Date of Contract: 1 May 1972
Contract Expiration Date: 31 December 1975
Amount of Contract: $598,861.00
Program Code Number: 5E20

Principal Investigator: J. Alex Thomson
Phone: 415 848-3063

Project Engineer: Richard Carman
Phone: 315 330-3085

Contracting Officer: Robert J. Hawkins
Phone: 315 330-4903

This research was supported by the Defense Advanced Research Projects Agency of the Department of Defense and was monitored by Richard Carman RADC(OCSE), GAFB NY 13441 under Contract F30602-72-C-0494, Job Order No. 16490402.

This report has been reviewed by the RADC Information Office (OI), and is releasable to the National Technical Information Service (NTIS).

This technical report has been reviewed and is approved.

RADC Project Engineer

UNCLASSIFIED

SECURITY CLASSIFICATION OF THIS PAGE (When Data Entered)

REPORT DOCUMENTATION PAGE		READ INSTRUCTIONS BEFORE COMPLETING FORM
1. REPORT NUMBER RADC-TR-75-	2. GOVT ACCESSION NO. AD-A955 300	3. RECIPIENT'S CATALOG NUMBER
4. TITLE (and Subtitle) Nonlinear Interaction of a Narrow Surface Spectrum with a Prescribed Surface Current		5. TYPE OF REPORT & PERIOD COVERED Scientific 6. PERFORMING ORG. REPORT NUMBER PD-75-072
7. AUTHOR(s) Kenneth M. Watson Bruce J. West		8. CONTRACT OR GRANT NUMBER(s) F30602-72-C-0494
9. PERFORMING ORGANIZATION NAME AND ADDRESS Physical Dynamics, Inc. P. O. Box 1069 Berkeley, CA 94701		10. PROGRAM ELEMENT, PROJECT, TASK AREA & WORK UNIT NUMBERS
11. CONTROLLING OFFICE NAME AND ADDRESS ARPA/STO 1400 Wilson Blvd Arlington, VA 22209		12. REPORT DATE Jure 6, 1975 13. NUMBER OF PAGES 56
14. MONITORING AGENCY NAME & ADDRESS(if different from Controlling Office) RADC/OCSE ATTN: Leonard Strauss Griffiss AFB, NY 13441		15. SECURITY CLASS. (of this report) Unclassified 15a. DECLASSIFICATION/DOWNGRADING SCHEDULE

16. DISTRIBUTION STATEMENT (of this Report)

Approved for public release; distribution unlimited

17. DISTRIBUTION STATEMENT (of the abstract entered in Block 20, if different from Report)

18. SUPPLEMENTARY NOTES

19. KEY WORDS (Continue on reverse side if necessary and identify by block number)

20. ABSTRACT (Continue on reverse side if necessary and identify by block number)

Envelope solitons for surface waves in deep water are studied using the coupled equation for the Fourier amplitudes of the surface displacement. Comparison is made with some wave-tank experiments of Feir. A linear stability analysis is made for an imposed transverse ripple. A slowly growing instability is found at wavelengths comparable to, or longer than, the length of the soliton. A slowly developing instability is found also for a soliton propagating through a train of waves of wavelength appreciably smaller

DD FORM 1 JAN 73 1473 EDITION OF 1 NOV 65 IS OBSOLETE

UNCLASSIFIED

SECURITY CLASSIFICATION OF THIS PAGE (When Data Entered)

20. ABSTRACT

than that of the soliton. A soliton propagating through a train of waves with wave-length much larger than that of the soliton exhibits gross distortion due to the orbital fluid velocity of the wavetrain. This distortion is to some extent reversible, as the soliton tends to "recover" when the wave-train is damped to zero amplitude.

TABLE OF CONTENTS

NONLINEAR INTERACTION OF A NARROW SURFACE SPECTRUM WITH A PRESCRIBED SURFACE CURRENT

Bruce J. West

Physical Dynamics, Inc.
P. O. Box 1069
Berkeley, California

and

Bruce I. Cohen and Kenneth M. Watson

Department of Physics and Lawrence Berkeley Laboratory
University of California, Berkeley, California 94720

June 6, 1975

ABSTRACT

Envelope solitons for surface waves in deep water are studied using the coupled equation for the Fourier amplitudes of the surface displacement. Comparison is made with some wave-tank experiments of Feir. A linear stability analysis is made for an imposed transverse ripple. A slowly growing instability is found at wavelengths comparable to, or longer than, the length of the soliton. A slowly developing instability is found also for a soliton propagating through a train of waves of wavelength appreciably smaller than that of the soliton. A soliton propagating through a train of waves with wave-length much larger than that of the soliton exhibits gross distortion due to the orbital fluid velocity of the wavetrain. This distortion is to some extent reversible, as the soliton tends to "recover" when the wavetrain is damped to zero amplitude.

1. INTRODUCTION

In this report we discuss the effect of the nonlinear terms in the eigenmode equations given by West, Watson and Thomson (1974)* on the evolution of a narrow spectrum of gravity waves on the ocean surface. This spectrum produces an envelope of a carrier wavenumber k_M and the nonlinear equation of evolution of the envelope is found to have the form of a nonlinear Schrödinger equation, as discussed by Davey (1972). The envelope represents a wavepacket propagating on the ocean surface. The propagation of a symmetric wavepacket of deep water waves was studied by Lighthill (1965,1967). In his analysis nonlinear interactions led to the development of a nonsymmetric shape and a peaking of the packet envelope function. The relation between the eigenmode equations and the averaged Lagrangian technique developed by Whitham (1965,1967) for water waves is also discussed.

That certain waveforms have a persistent shape due to the balancing of nonlinear and dispersive effects has been observed by Benney and Newell (1967). Experimental studies of such wavetrains propagating in wave tanks have been reported by Feir (1965) and by Lake and Yuen (1975). The observed properties of these wave systems seem to be consistent with theoretical expectations [e.g. see, Chu and Mei (1970, (1971)]. The Nonlinear Schrödinger equation describes

---

*This reference will hereafter be referred to as I or Part I.

the space time evolution of the envelope function of a narrow bandwidth train of deep water waves. It is shown in Section 2 that the nonlinear Schrödinger equation has soliton solutions for an initially narrow spectrum as discussed by Kadomtsev and Karpman (1971) and Zakharov and Shabat (1972).

The effect of spectral broadening on the nonlinear interaction is investigated numerically using the code developed in Part I. In I the authors make a numerical analysis of the coupled mode equations describing the nonlinear interaction of surface gravity waves. In this analysis a tendency for "bumps" in the envelope of a wavetrain to grow was noted. Indeed, unless care was taken to avoid such "bumps" in selecting the initial conditions, the growth of these tended to obscure the other phenomena being studied.

In Section 2 the nonlinear Schrödinger equation is obtained as an approximation to the coupled mode equations. Solutions for envelope solitons and the Benjamin-Fier instability criteria will be noted for subsequent reference in Section 3. Some numerical examples of the propagation and distortion of solitons are also given in Section 3 and the calculated results are compared with observations from wavetanks.

Soliton stability is studied in Section 4. It is shown that a periodic modulation parallel to the wavecrests

causes a rather slowly growing instability. It is also shown that even in the one-dimensional case that the envelope soliton appears to be unstable upon encountering a second wavetrain of substantially different wave numbers than those of which the soliton is constructed. This does not violate the conclusions of Zakharov and Shabat (1972), ie., solitons are stable when interacting with other wavetrains described by the same nonlinear Schrodinger equation, since the two wavetrains of substantially different frequencies each satisfy different nonlinear Schrödinger equations.

2. THE EIGENMODE EQUATIONS

Consider a current at the ocean surface represented by a superposition of modes parallel to the x axis,

$$\underset{\sim}{U}(x,t) = \hat{i} \sum_{K} U_K \cos K\xi \qquad (2.1)$$

where $\xi = x - c_I t$, and c_I is the velocity of the current profile. Each mode in Eq. (2.1) has a wavelength $2\pi/K$ and amplitude U_K. The equation describing the linear interaction of a surface current of the form of Eq. (2.1) and the linear wave field at the ocean surface was found in Case, Watson and West (1974)*, to be of the form of a Schrödinger equation.

Following the notation of III we define the complex amplitude

$$Z(\vec{r},t) = \sum_{\vec{k}} a(\vec{k}) \exp(i\vec{k}\cdot\vec{r}) \qquad (2.2)$$

where $\vec{r} = (x,y)$ is a horizontal vector on the ocean surface. The surface elevation may be written in terms of the complex amplitudes as,

$$h(\vec{r},t) = - \mathrm{Im}\left[Z(\vec{r},t)\right]$$

$$= \frac{i}{2}\left[Z(\vec{r},t) - Z^*(\vec{r},t)\right] \quad . \qquad (2.3)$$

*This report will hereafter be referred to as III.

The equations describing the interaction between the surface wave field and the surface current are written in model form in Watson, West and Cohen (1973)*, in terms of the variable

$$c(\vec{k}) = a(\vec{k}) \exp(ik_x c_I t) \tag{2.4}$$

rather than $a(\vec{k})$. The wavenumber k_x is the horizontal wavenumber parallel to the surface current. The resonant coupled mode equations are,

$$i\dot{c}(\vec{k}) = (\omega_k - k_x c_I) c(\vec{k}) + \sum_K \left[A^{(-)}(\vec{k},\vec{K}) c(\vec{k}-\vec{K}) + A^{(+)}(\vec{k},\vec{K}) c(\vec{k}+\vec{K}) \right]$$

$$- \sum_{\vec{\ell},\vec{p},\vec{n}} \Gamma^{\vec{k}\vec{n}}_{\vec{\ell}\vec{p}} \, c(\vec{\ell}) c(\vec{p}) c^*(\vec{n}) \exp\left[i(k_x + n_x - \ell_x - p_x) c_I t \right] \delta_{\vec{k}+\vec{n}-\vec{\ell}-\vec{p}} \tag{2.5}$$

where the coupling coefficients $\Gamma^{\vec{k}\vec{n}}_{\vec{\ell}\vec{p}}$ are given in Part I, the $A^{(+)}(\vec{k},\vec{K})$ are given in II and the effects of wind, viscosity and surface tension have been neglected for the moment.

In III the linear part of Eq. (2.5) is reduced to the form

$$i \dot{\underset{\sim}{\psi}} = \underset{\sim}{H} \underset{\sim}{\psi} \tag{2.6}$$

where $\underset{\sim}{H}$ is a hermitian matrix and $\underset{\sim}{\psi}$ is related to $c(\vec{k})$ by a linear transformation. In the following sections

*This report will hereafter be referred to as II.

Eq. (2.6) will be generalized by keeping the nonlinear part of Eq. (2.5) in the analysis and constructing a nonlinear equation of evolution for the envelope function of an initially isolated wave.

2.1 THE ENVELOPE FUNCTION

If we define the x component of the surface waves to be in the direction of the current given by Eq. (2.1), then we may proceed as in III and parameterize the dependence of the surface wavenumber on the direction orthogonal to the current. We write the surface wavenumber as $k = \sqrt{k_x^2 + p^2}$, where p is a parameter. Further, since $k >> K$ for all surface waves of interest on the ocean, we write

$$k_x = nK \ , \qquad n = 1, 2, \ldots \tag{2.7}$$

so that the wavenumber component parallel to the current is a multiple of the surface current fundamental wavenumber (K).

Equation (2.7) allows us to rewrite Eq. (2.5) in terms of the discrete quantities

$$\psi(n) = \gamma_n^{-1} \ c(\vec{k}) \tag{2.8}$$

so that

$$i\dot{\psi}(n) = E_n\psi(n) + V_{n,n+1} \ \psi(n+1) + V_{n,n-1} \ \psi(n-1)$$

$$- \sum_{q,\ell,m} \delta_{q+n-\ell-m} \ \Gamma_{\ell m}^{nq} \ \gamma_q\gamma_\ell\gamma_m \ \psi^*(q)\psi(\ell)\psi(m) \ \exp\left[-i(\ell+m-q-n)\Omega t\right] \tag{2.9}$$

where

$$E_n \equiv \omega_n - n\Omega \quad ,$$

$$V_{n,n+1} = \frac{\gamma_{n+1}}{\gamma_n} A^{(+)}(n) \quad ,$$

$$V_{n,n-1} = \frac{\gamma_{n-1}}{\gamma_n} A^{(-)}(n) \quad , \tag{2.10}$$

$\omega_n = \omega_{|\vec{k}|}$, and Ω is the frequency of the surface current ($\equiv Kc_I$). If we now choose the transformation coefficients to be

$$\gamma_{n-1}/\gamma_n \equiv \left[A^{(+)}(n-1)/A^{(-)}(n)\right]^{\frac{1}{2}} \tag{2.11}$$

so that

$$V_{n,n+1} = \sqrt{A^{(+)}(n)\ A^{(-)}(n+1)}$$

$$V_{n,n-1} = \sqrt{A^{(+)}(n-1)\ A^{(-)}(n)} \tag{2.12}$$

the matrix $\underset{\sim}{V}$ will be symmetric. Equation (2.9) now has the form

$$i\,\dot{\underset{\sim}{\psi}}(n) = \left[(\underset{\sim}{K}+\underset{\sim}{V})\,\underset{\sim}{\psi}\right](n)$$

$$- \sum_{\ell,m,q} \delta_{q+n-\ell-m}\ \Gamma^{nq}_{\ell m}\ \frac{\gamma_q \gamma_\ell \gamma_m}{\gamma_n}\ \psi(\ell)\,\psi(m)\,\psi^*(q)\exp\left[i\,(n+q-\ell-m)\Omega\,t\right] \tag{2.13}$$

the linear part of which is given by Eq. (2.6), with

$$K_{nn'} = E_n \, \delta_{nn'} \quad .$$

If we consider a solution to Eq. (2.13) of the form

$$\psi(n,t) \equiv \frac{Q^{(M)}}{\sqrt{2}\ \gamma_M} \Phi(n,t)\ \exp(-iE_M t) \tag{2.14}$$

which is a simple wave of wavenumber k_M at $t = 0$

$$\psi(n,t=0) = \delta_{n,M}\ Q^{(M)}/\sqrt{2}\ \gamma_M \quad ,$$

i.e., $\lim_{t\to 0} \Phi(n,t) \to \delta_{nM}$, we obtain from Eq. (2.13)

$$i\ \dot{\Phi}(n) = (E_n - E_M)\ \Phi(n) + V_{n,n+1}\ \Phi(n+1) + V_{n,n-1}\ \Phi(n-1)$$

$$- \sum_{n+q=\ell+m} \tfrac{1}{2}\ \Gamma^{nq}_{\ell m} \left[\frac{Q^{(M)}}{\gamma_M}\right]^2 \frac{\gamma_\ell \gamma_m \gamma_q}{\gamma_n}\ \Phi(\ell)\,\Phi(m)\,\Phi^*(q)\ \exp\left[-i\,(n+q-\ell-m)\,\Omega t\right] \quad . \tag{2.15}$$

Using the complex amplitude defined by Eq. (2.2), the relations (2.4) and (2.8) and from II

$$c(\vec{k}) \equiv q_{\vec{k}}\ \exp(-i\omega_k t)/\sqrt{2} \tag{2.16}$$

we may write

$$Z(\vec{r},t) = \sum_{\vec{k}_n} \sqrt{2}\, \frac{\gamma_n\ \psi(n)}{k_n} \exp\left[i(\vec{k}_n\cdot\vec{r}-n\Omega t)\right] \qquad (2.17)$$

where $k_n \equiv \sqrt{(nK)^2 + p^2}$. In terms of the solutions (2.14), Eq. (2.17) can be written

$$Z(\vec{r},t) = \frac{Q^{(M)}}{k_M} \exp\left[i(k_M\xi-\omega_M t)\right] \sum_{\Delta n} \frac{k_M\ \gamma_n}{k_n\ \gamma_M}\, \Phi(n,t)\ \exp\left[i\Delta nK(\xi-c_g^{(M)}t)\right] \qquad (2.18)$$

where $\Delta n = n-M$, $\xi = x - c_I t$ and $c_g^{(M)}$ is the group velocity of the central mode. The sum on the right-hand side of Eq. (2.18) defines the envelope function for the initial wave, i.e.,

$$G^{(M)} \equiv \sum_{\Delta n} \frac{k_M\ \gamma_n}{k_n\ \gamma_M}\, \Phi(n,t)\ \exp(i\Delta nK\xi') \qquad (2.19)$$

and is expected to be slowly varying ($\xi' = x - (c_I+c_g^{(M)})t$).

The evolution of the surface modulation can be obtained from the dynamic equation for the envelope function. Taking the derivative of $G^{(M)}$ with respect to time yields,

$$\frac{\partial G^{(M)}}{\partial t} = \sum_n \frac{k_n\ \gamma_n}{k_n\ \gamma_M} \left[-i\Delta nKc_I\,\Phi(n) + \frac{\partial\Phi(n)}{\partial t}\right]\exp(i\Delta nK\xi)$$

or equivalently,

$$i\left(\frac{\partial}{\partial t} + c_I\,\frac{\partial}{\partial x}\right) G^{(M)} = \sum_n \frac{k_n\ \gamma_n}{k_n\ \gamma_M} \exp(i\Delta nK\xi)\ i\frac{\partial\Phi(n)}{\partial t}\ . \qquad (2.20)$$

Equation (2.20) may be evaluated by substitution from Eq. (2.15).

To simplify the nonlinear term in Eq. (2.15) we rewrite the restriction on the sum in the integral form

$$\frac{1}{W} \int_0^W \exp\left[i(\vec{n}+\vec{q}-\vec{\ell}-\vec{m}) \cdot \vec{r} \right] d^2 r \quad .$$

over the area of ocean W. If we further assume the nonlinear interaction to be local, so that the interaction coefficient is strongly peaked about k_M, we set $\Gamma^{(M)} \equiv \frac{k_\ell k_m k_q}{k_n} \Gamma^{nq}_{\ell m}$ to be a constant. The cubic term in Eq. (2.20) may then be expressed as

$$- \frac{1}{2} \left(\frac{Q^{(M)}}{k_M} \right)^2 \sum_{\ell,m,q} \Gamma^{(M)} \left(\frac{k_M}{\gamma_M} \right)^3 \frac{\gamma_\ell}{k_\ell} \Phi(\ell) \exp(i\Delta\ell k \xi) \frac{\gamma_m}{k_m} \Phi(m)$$

$$\exp(i\Delta m K \xi) \frac{\gamma_q}{k_q} \Phi^*(q) \exp(-i\Delta q K \xi)$$

and using the definition of the modulation function, Eq. (2.20) reduces to

$$i \left\{ \frac{\partial}{\partial t} + c_I \frac{\partial}{\partial x} \right\} G^{(M)} = - C^{(M)} |G^{(M)}|^2 G^{(M)}$$

$$+ \sum_{\Delta n} \frac{k_M \gamma_n}{k_n \gamma_M} \left\{ (E_n - E_M) \Phi(n) + V_{n,n+1} \Phi(n+1) + V_{n,n-1} \Phi(n-1) \right\}$$

$$\times \exp(i\Delta n K) \quad . \qquad (2.21)$$

The cubic coupling coefficient is given by

$$C(M) \equiv \frac{1}{2}\left(\frac{Q^{(M)}}{k_M}\right)^2 \Gamma^{(M)}$$

so that using the diagonal nonlinear coupling coefficient $\Gamma^{MM}_{MM} = -\omega_M$ from Part I since equations are in terms of slopes, we have

$$C^{(M)} = -\frac{1}{2}\,\omega_M \left[Q^{(M)}\right]^2 \tag{2.22}$$

We can expand the diagonal matrix elements of the Hamiltonian $(K+V)(n)$ about $n = M$ to obtain

$$E_n - E_M = (n-M)\,\frac{\partial E_n}{\partial n} + \frac{(n-M)^2}{2}\,\frac{\partial^2 E_n}{\partial n^2} + \ldots.$$

Using this expansion allows us to sum the first series in (3.14), i.e,

$$\sum_{\Delta n} \frac{k_M \gamma_n}{k_n \gamma_M}\,(E_n - E_M)\,\Phi(n,t)\exp(i\Delta n K\xi) \approx -i\,\frac{\partial E_M}{\partial k_M}\,\frac{\partial G^{(M)}}{\partial x} - \frac{1}{2}\,\frac{\partial^2 E_M}{\partial k_M^2}\,\frac{\partial^2 G^{(M)}}{\partial x^2} + \ldots \tag{2.23}$$

The second series may be summed in a similar manner when the current has a harmonic decomposition, i.e.,

$$\sum_{\Delta n}\left[V_{n,n+1}\Phi(n+1) + V_{n,n-1}\Phi(n-1)\right]\exp(i\Delta n K\xi) = k_M U\,G^{(M)} - i\frac{\partial}{\partial x}\left[UG^{(M)}\right]. \tag{2.24}$$

Since $E_M = \omega_M - M\Omega$, we have

$$\frac{\partial E_M}{\partial k_M} = \omega'_M - \frac{\Omega}{K} = c_g^{(M)} - c_I, \tag{2.25}$$

the difference between the group velocity of the central mode and the phase velocity of the current pattern. Using Eqs. (2.23) - (2.25) in (2.21) yields

$$i\left\{\frac{\partial}{\partial t} + (\omega_M'+U)\frac{\partial}{\partial x} + \frac{\partial U}{\partial x}\right\} G^{(M)} = -\frac{1}{2}\omega_M''\frac{\partial^2 G^{(M)}}{\partial x^2} + \left[k_M U - C^{(M)}|G^{(M)}|^2\right] G^{(M)} \tag{2.26}$$

where $\omega_M'' = \dfrac{d^2\omega_M}{dk_M^2}$.

Equation (2.26) is the equation of evolution for the envelope function $G^{(M)}$. In the absence of a current and in a coordinate system translating with the group velocity $c_g^{(M)}$, i.e., $\xi = x - c_g^{(M)} t$, Eq. (2.26) can be written

$$i\frac{\partial G^{(M)}}{\partial t} = -\frac{1}{2}\omega_M''\frac{\partial^2 G^{(M)}}{\partial \xi^2} - C^{(M)}|G^{(M)}|^2 G^{(M)} \tag{2.27}$$

which is immediately identified as a nonlinear Schrödinger equation. The discussions leading to Eq. (2.27) have been varied, some based on scaling arguements, e.g., Diprima, et al. (1971), Benney and Newell (1967), and more recently on the averaged Lagrangian approach of Whitham, e.g., Lake and Yuen (1975). This later approach was also used taking into account dissipation by Davey (1972) to derive (2.27).

In addition to the wave-wave nonlinear interaction, the current interaction and the dispersive effects of the wave field, we introduce a linear model for the generation of waves by wind and their viscous decay

$$\alpha_M \equiv k_M^2 \left[\frac{\mu}{2\,\omega_M} \operatorname{sign}(k_M) - \nu \right] \tag{2.28}$$

where μ and ν are the wind and viscosity coupling strengths respectively. Including these terms in the equation of evolution of the envelope function yields

$$i\left\{ \frac{\partial}{\partial t} + (\omega_M' + U)\ \frac{\partial}{\partial x} + \frac{\partial U}{\partial x} - \alpha_M + C_I^{(M)} |G^{(M)}|^2 \right\} G^{(M)} + \frac{1}{2}\,\omega_M''\, G^{(M)}$$

$$= \left[k_M U - C_R^{(M)}\ |G^{(M)}|^2 \right] G^{(M)} \quad . \tag{2.29}$$

The nonlinear coupling coefficient is imaginary in the non-conservative system, i.e., $C^{(M)} \equiv C_R^{(M)} + i\, C_I^{(M)}$. Note that the wind coupling model is intended to demonstrate the effect and not to provide a "realistic" generation term for the wind. In calculations this term would be replaced by the Phillips-Miles linear model of wind coupling to the air-sea interface.

2.2 THE CONSERVATIVE SYSTEM

Consider the form of Eq. (2.28) for an inviscid fluid in the absence of wind and with no current present. If we also suppress the index of the central mode (M) then

$$i\left\{\frac{\partial G}{\partial t} + \omega' \frac{\partial G}{\partial x}\right\} + \frac{1}{2}\omega'' \frac{\partial^2 G}{\partial x^2} + C|G|^2 G = 0 \quad . \tag{2.30}$$

Assume a solution to Eq. (2.30) of the form

$$G(x,t) = A(x,t) \exp\left[i\Phi(x,t)\right] \tag{2.31}$$

where A and Φ are real. Using (2.31) in (2.30) and equating real and imaginary parts yields

$$A_{xx} - \Phi_x^2 A - \frac{2}{\omega''}\left[\Phi_t + \omega' \Phi_x - CA^2\right]A = 0$$

$$\left[\Phi_x A^2\right]_x + \frac{2}{\omega''}\left[A_t + \omega' A_x\right]A = 0 \tag{2.32}$$

where the subscript notation for partial derivatives has been adopted and ' denotes a derivative with respect to k.

We identify the derivatives of the phase function with a wavenumber (κ) and frequency (Ω),

$$\kappa = \Phi_x \quad ; \quad \Omega = -\Phi_t \tag{2.33}$$

so that (2.32) becomes

$$A_{xx} - \kappa^2 A - \frac{2}{\omega''}\left[-\Omega + \kappa\omega' - CA^2\right]A = 0$$

$$\left[\kappa A^2\right]_x + \frac{2}{\omega''}\left[A_t + \omega' A_x\right]A = 0 \quad . \tag{2.34}$$

The first of Eq. (2.34) can be integrated under the assumption that κ and Ω are constant to yield

$$(A_x)^2 = \frac{2}{\omega''}\left[-\Omega + \kappa\omega' + \frac{1}{2}\kappa^2\omega'' - \frac{1}{2}CA^2\right]A^2 \quad . \tag{2.35}$$

The solution to Eq. (2.35) is

$$A = A_o \operatorname{sech} B(t - x/v_g) \tag{2.36}$$

with

$$\Omega = \kappa\omega' + \frac{1}{2}\kappa^2\omega'' - \frac{1}{2}CA_o^2$$

$$B = \left(\frac{C}{\omega''}\right)^{\frac{1}{2}} A_o v_g \quad . \tag{2.37}$$

From the second expression in Eq. (2.34) we have

$$A_t + (\omega' + \kappa\omega'')A_x = 0 \tag{2.38}$$

so that the amplitude is constant along the trajectory

$$\frac{dx}{dt} \equiv v_g = \omega' + \kappa\,\omega'' \quad . \tag{2.39}$$

The solution to Eq. (2.30) is therefore

$$G(x,t) = A_o\ \mathrm{sech}\left[\left(\frac{C}{\omega''}\right)^{\frac{1}{2}} A_o (x - v_g t)\right]\ \exp\, i(\kappa x - \Omega t) \tag{2.40}$$

which is both localized and stationary as discussed by Hasegawa and Tappert (1973a,b). The quantity $\left(\frac{C}{\omega''}\right)^{\frac{1}{2}}$ is seen from Eq. (2.22) to be related to the slope of the central mode $\left[\sqrt{2}\ k_M\ Q^{(M)}\right]$, so that again using indices we have

$$G^{(M)}(x,t) = A_o\ \mathrm{sech}\left[\sqrt{2}\ k_M\ Q^{(M)} A_o (x - v_g^{(M)}\ t)\right]\ \exp\, i\left[\kappa_M x - \Omega_M t\right] \quad . \tag{2.41}$$

3 STABILITY OF FINITE AMPLITUDE WAVES

In a now classic experiment, Benjamin and Feir (1967) mechanically generated a wave of fairly large slope (.17) on the surface of a water tank. Perturbations of this wave located at sidebands of the initial wavenumber induced a modulation of the generated wave. The location of these sidebands were determined from a perturbation analysis and found to grow exponentially out of the background noise in the surface wave spectrum. This instability was observed experimentally as a randomization of the finite amplitude wave some distance from the wave source. A numerical calculation of this break up process using the third order nonlinear modal equations was done in Part I for deep water waves.

Hasimoto and Ono (1972) have shown, using a perturbation expansion of the dynamic equations for water waves, that the envelope function of the first order surface wave amplitude satisfies an equation of the form (2.30). Their analysis indicates that a nonlinear plane wave solution to Eq. (2.30) yields a second order Stokes wave profile for the surface elevation. The critical results of Benjamin (1966) and Whitham (1967) for shallow water wave profile for reproduced, i.e., the dynamic equation changes character from elliptic ($Kh_o < 1.36$) to hyperbolic ($Kh_o > 1.36$) where K is the wavenumber of the wave train and h_o is the depth of the water.

Whitham (1967) determined that the coupled modulations of the phase and amplitude in the averaged Lagrangian approach is equivalent to the sideband modulation used by Benjamin (1966) and later by Benjamin and Fier (1967). Recently, Lake and Yuen (1975) have shown that Eq. (2.30) can be derived from an averaged Lagrangian when the spatial variation in the envelope function is not neglected. One may also derive Eq. (2.32) in a coordinate system translating with the velocity ω', i.e., $\xi = x-\omega' t$, from the Lagrangian.

$$L = \frac{1}{2}\left[\left(\frac{\partial A}{\partial \xi}\right)^2 + A^2\left(\frac{\partial \Theta}{\partial \xi}\right)^2\right] + \frac{1}{\omega''}\frac{\partial \Theta}{\partial t}A^2 - \frac{C}{2\omega''}A^4 \tag{3.1}$$

where A and Θ are defined in Eq. (2.31). The equations of motion are obtained from the variation

$$\delta \int L\left[A, \frac{\partial A}{\partial \xi}, \frac{\partial A}{\partial t}, \Theta, \frac{\partial \Theta}{\partial \xi}, \frac{\partial \Theta}{\partial t}\right] dxdt = 0 \tag{3.2}$$

to be

$$\frac{\partial}{\partial t}\left[\frac{\partial L}{\partial\left(\frac{\partial A}{\partial t}\right)}\right] + \frac{\partial}{\partial \xi}\left[\frac{\partial L}{\partial\left(\frac{\partial A}{\partial \xi}\right)}\right] = \frac{\partial L}{\partial A}$$

$$\frac{\partial}{\partial t}\left[\frac{\partial L}{\partial\left(\frac{\partial \Theta}{\partial t}\right)}\right] + \frac{\partial}{\partial \xi}\left[\frac{\partial L}{\partial\left(\frac{\partial \Theta}{\partial \xi}\right)}\right] = \frac{\partial L}{\partial \Theta} \cdot \tag{3.4}$$

Equation (3.4), using (3.1) is identical to Equation (2.32). This system behaves like a particle under the influence of

a central potential of the form

$$V(A, \theta) = -\frac{1}{\omega''}\frac{\partial\theta}{\partial t} A^2 + \frac{C}{2\omega''} A^4 \qquad (3.5)$$

as discussed by Watanabe (1969).

To examine the instability of the finite amplitude wave, we extend the arguments of Hasimoto and Ono slightly and consider the envelope function

$$G(x,t) = (A_o + \varepsilon A^{(1)}) \exp i(\kappa x - \Omega t + \varepsilon\theta) \qquad (3.6)$$

where A_o, κ and Ω are constants, $A^{(1)}$ and θ are functions of x and t, and ε is a smallness parameter. Substituting Eq. (3.6) into (2.30) and linearizing with respect to ε yields,

$$A_t^{(1)} + \frac{1}{2}\omega'' A_o \theta_{\xi\xi} = 0$$

$$A_o\theta_t - \frac{1}{2}\omega'' A_{\xi\xi}^{(1)} - 2CA_o^2 A^{(1)} = 0 \qquad (3.7)$$

where it is determined that

$$\Omega = \kappa\omega' + \frac{1}{2}\kappa^2\omega'' - CA_o^2 \qquad (3.8)$$

as found in Section 2.2. Equation (3.7) is defined in a coordinate system translating with a velocity $\omega' + \kappa\omega''$, i.e., $\xi = x - (\omega' + \kappa\omega'')t$.

To determine the stability of the solutions to Equation (3.7), we substitute the second equation into the partial time derivative of the first to obtain

$$A_{tt}^{(1)} + \left(\frac{1}{2}\omega''\right)^2 A_{\xi\xi\xi\xi}^{(1)} + \omega'' C A_o^2 A_{\xi\xi}^{(1)} = 0 \ . \qquad (3.9)$$

A solution to Equation (3.9) of the form $\exp[i(k_1 x - \omega_1 t)]$ yields the dispersion relation

$$\omega_1^2 = \left(\omega''\frac{k_1}{2}\right)^2 \left(k_1^2 - 4C A_o^2/\omega''\right) \qquad (3.10)$$

which, since $C/\omega'' > 0$, has unstable solutions when

$$2A_o \sqrt{C/\omega''} > k_1 \ . \qquad (3.11)$$

Using the value of C/ω'' obtained in Section 2.2, we have the condition

$$(2)^{3/2} A_o k_M Q^{(M)} > k_1 \qquad (3.12)$$

where $Q^{(M)}$ and k_M are the initial slope and wavenumber of the central mode.

Condition (3.11) is just that obtained by Benjamin and Fier (1967) for the stability of a finite amplitude wave. The amplitude of the sideband (a_1) grows like

$$a_1 \sim \exp(\gamma t)$$

where from Eq. (3.10)

$$\gamma = \frac{1}{2}\,\omega_M \left\{ 2\left[Q^{(M)} A_o\right]^2 - \delta^2 \right\}^{1/2} \delta \qquad (3.13)$$

with ω_M the frequency and $Q^{(M)}$ the initial slope of the central mode, and δ the fractional change in the frequency induced by the nonlinearity. Taking the variation of γ with δ, we determine $\delta_{max} = Q^{(M)} A_o$, so that the initial slope of the central mode determines the position of the sidebands receiving maximum amplification, i.e., $\omega_\pm = \left[1 \pm Q^{(M)} A_o\right]\omega_M$ and $k_\pm = \left[1 \pm 2Q^{(M)} A_o\right]k_M$. At these wavenumbers the growth rate is

$$\gamma = \pm \sqrt{2}\ \omega_k (KA_o)^2 \quad .$$

On writing $m = KA_o$ for the slope of the large amplitude wave, we see that

$$\tau_{BF} \equiv (\sqrt{2}\ \omega_k\ m^2)^{-1} \qquad (3.14)$$

describes an e-folding time for the Benjamin-Feir interaction. Reference to the nonlinear term in Eq. (2.5) suggests that τ_{BF} can be taken as a characteristic time scale for nonlinear interactions to develop.

3.1 COMPARISON WITH THE FEIR EXPERIMENTS

The numerical code described in Part I integrates Eqs. (2.5) for a specified set of modes, but is restricted to one-dimension, with all wavenumbers parallel to, say the x-axis. A "fetch" L is specified with periodic boundary conditions at $x = -\frac{L}{2}$ and $x = \frac{L}{2}$. The mode spacing is $\Delta k = 2\pi/L$.

To integrate Eqs. (2.5) with $c_I=0$, ie., no external current, the initial amplitudes $a_n(0)$ ($k_n = n\Delta k$, n = 1, 2, ...) at t = 0 are specified.

If the initial state of Eq. (2.5) is prepared to be that of a soliton, then the nonlinear interactions should not change the surface structure, i.e., the soliton should persist as it propagates along the water surface. The initial conditions for Eq. (2.5) are obtained by taking the Fourier transform of the envelope function at time t = 0, to obtain the mode amplitudes

$$a_n(0) = \frac{1}{L} \int_{-\infty}^{\infty} G(\xi,0) \exp\left[i(K - k_n)\ \xi\right] d\xi \quad , \tag{3.15}$$

where $G(\xi,0)$ is given in Eq. (2.41). Integrating and normalizing Eq. (3.15), we obtain for the mode amplitudes of an initial soliton

$$a_n(0) = a_N(0)\ \text{sech}\left[\frac{(N - n)\ \pi\Delta k}{\sqrt{8}\ \ m\ K}\right] \tag{3.16}$$

with the central mode given by wavenumber $K = N\Delta k$ and m the slope of the soliton.

In calculations, Eq. (3.16) is used to represent the initial soliton by a finite number of modes. In Figure 1a is shown an envelope function constructed from fifteen modes with the parameters, $K = 0.2516\ cm^{-1}$, $\Delta k = 0.01\ cm^{-1}$ and $m = 0.064$, where m is the slope of the soliton. This envelope is given by the absolute value of

$$G(x,t) = \sum_{n} \frac{q_n(t)}{k_n} \exp\left[i(N - n)\Delta k(x - c_g t)\right] \qquad (3.17)$$

where

$$c_g \equiv (\omega_n - \omega_N)/\Delta k(N - n)$$

is the group velocity of the central mode and the slope variables from Eq. (2.16) have been used. The modal rate equations in Part I are written in terms of the mode slopes, i.e., the q's, so that in Fig. 1 and in all subsequent figures involving the envelope, it is the absolute value of Eq. (3.17) that is plotted. The mode slopes for Fig. 1 are listed in Table I.

In Fig. 1b the displacement of the water surface is depicted for the above soliton. The surface displacement is described by Eqs. (2.2) and (2.3). The parameters for this example were selected to correspond to the wavepulse experiments conducted by Feir (1965). The initial amplitude of the central mode in Eq. (3.16) is obtained from the experiment using the expression

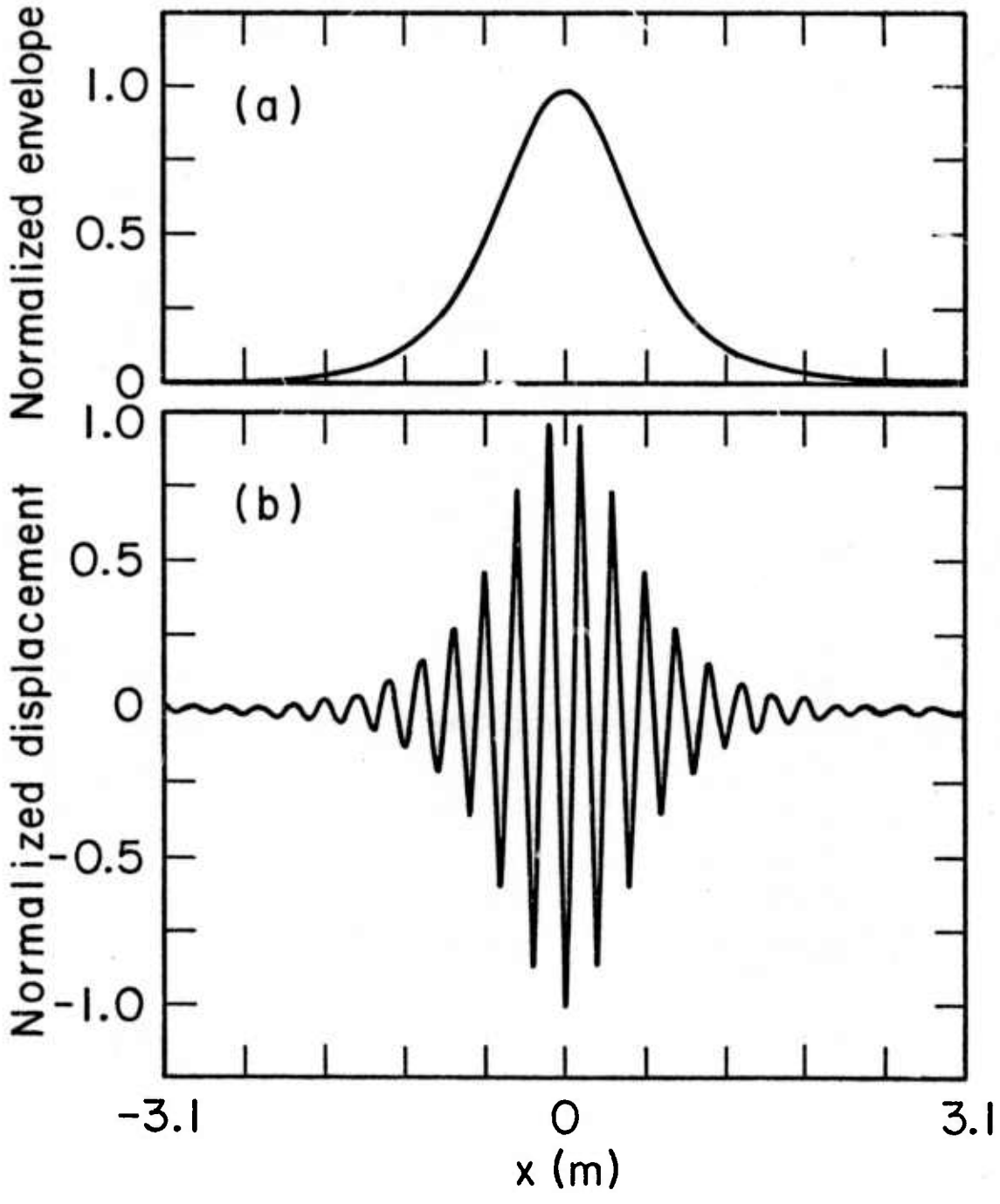

XBL756-3277

Fig. 1

TABLE I: Slope amplitudes [see Eq. (3.16)] for the "solitons" studied.

Mode Number n - N	Mode Slope Amplitudes of Solitons -- $q_n(0)$	
-7	10^{-5}	4×10^{-5}
-6	2.33×10^{-4}	9.32×10^{-4}
-5	5.36×10^{-4}	2.14×10^{-3}
-4	$1.2. \times 10^{-3}$	4.84×10^{-3}
-3	2.66×10^{-3}	1.06×10^{-2}
-2	5.6×10^{-2}	2.24×10^{-2}
-1	1.03×10^{-2}	4.12×10^{-2}
0	1.41×10^{-2}	5.64×10^{-2}
1	1.22×10^{-2}	4.88×10^{-2}
2	7.73×10^{-3}	3.09×10^{-2}
3	4.34×10^{-3}	1.74×10^{-2}
4	2.34×10^{-3}	9.36×10^{-2}
5	1.25×10^{-3}	5.0×10^{-3}
6	6.64×10^{-4}	2.66×10^{-3}
7	3.5×10^{-4}	1.4×10^{-3}
Viscosity coefficient-v	0.47 cm^2/sec	0.19 cm^2/sec
Soliton Slope-m	0.064	0.256
Central Wavenumber-K	0.2516 cm^{-1}	0.2516 cm^{-1}
Mode Spacing- k	0.01 cm^{-1}	0.01 cm^{-1}
Nonlinear Growth time-τ_{BF}	11.0 sec	0.69 sec

$$a_N(0) = G(x=0) \left\{ \sum_n \operatorname{sech}\left[\pi \Delta k (n - N)/\left(\sqrt{8}\ mK\right)\right] \right\}^{-1} \tag{3.18}$$

where m = 0.064 and G(x = 0) = 0.254 cm for the first trace in Fig. 3 of Feir (1965) yielding $a_N(0)$ = 0.056 cm. The slope of the soliton is given by the sum of the mode slopes, i.e.,

$$m = K \sum_n \frac{q_n(0)}{k_n} \tag{3.19}$$

which is also equal to the central wavenumber times the maximum surface displacement.

Figure 1 analytically models the shape of the pulse generated in Feir's experiment as measured four feet from the wavemaker. At a distance of twenty-four feet from this point, i.e., twenty-eight feet down the tank, the pulse amplitude is one half its initial value. This damping of the pulse is simulated in the present calculation using a phenomenological viscosity coefficient in the rate equations. The linear amplitude damping coefficient yields

$$G(x,t) = G(x,0) \exp(-\alpha t) \tag{3.20}$$

where t is given by the ratio of the distance traveled to the group velocity. The decay rate is given by α = 0.03 sec^{-1}, or in terms of the viscosity coefficient $\nu \equiv \alpha/K^2$ = 0.47 cm^2/sec.

Feir's discussion does not include the concept of a soliton. The analysis of Chu and Mei, (1970) however, compares the evolution of the pulse modeled as a soliton with the experimental results. As they pointed out the dominant effect is the attenuation in amplitude due to the short time of evolution; i.e., short compared with the e-folding time which is given in Table I as 11 sec. In Fig. 2 the results of the present calculation are given for the pulse after 24 seconds or approximately 24 feet from the initial point. The shape of the pulse is virtually unchanged from Fig. 1. The normalization has changed from 0.254 cm, however, to 0.115 cm; a 0.45 reduction in amplitude.

Feir describes the launching of six pulse shapes, all with the same central mode number and length of modulation, but with increasing amplitudes. The simulation of run (1), shown in Figs. 1 and 2, indicates that this pulse is very close to a soliton in shape. The remaining runs, with their increased amplitudes, must therefore not be solitons. The modulation instability of these waveforms causes these pulses to breakup into one or more stable solitons as discussed by Hasimoto and Ono (1972). This interpretation is consistent with what is observed in the latter runs of Feir [1965].

In Fig. 3 the last of the six runs from Feir (1965) is simulated. Since only the amplitude was increased between this and the first run, the mode slopes of the soliton are

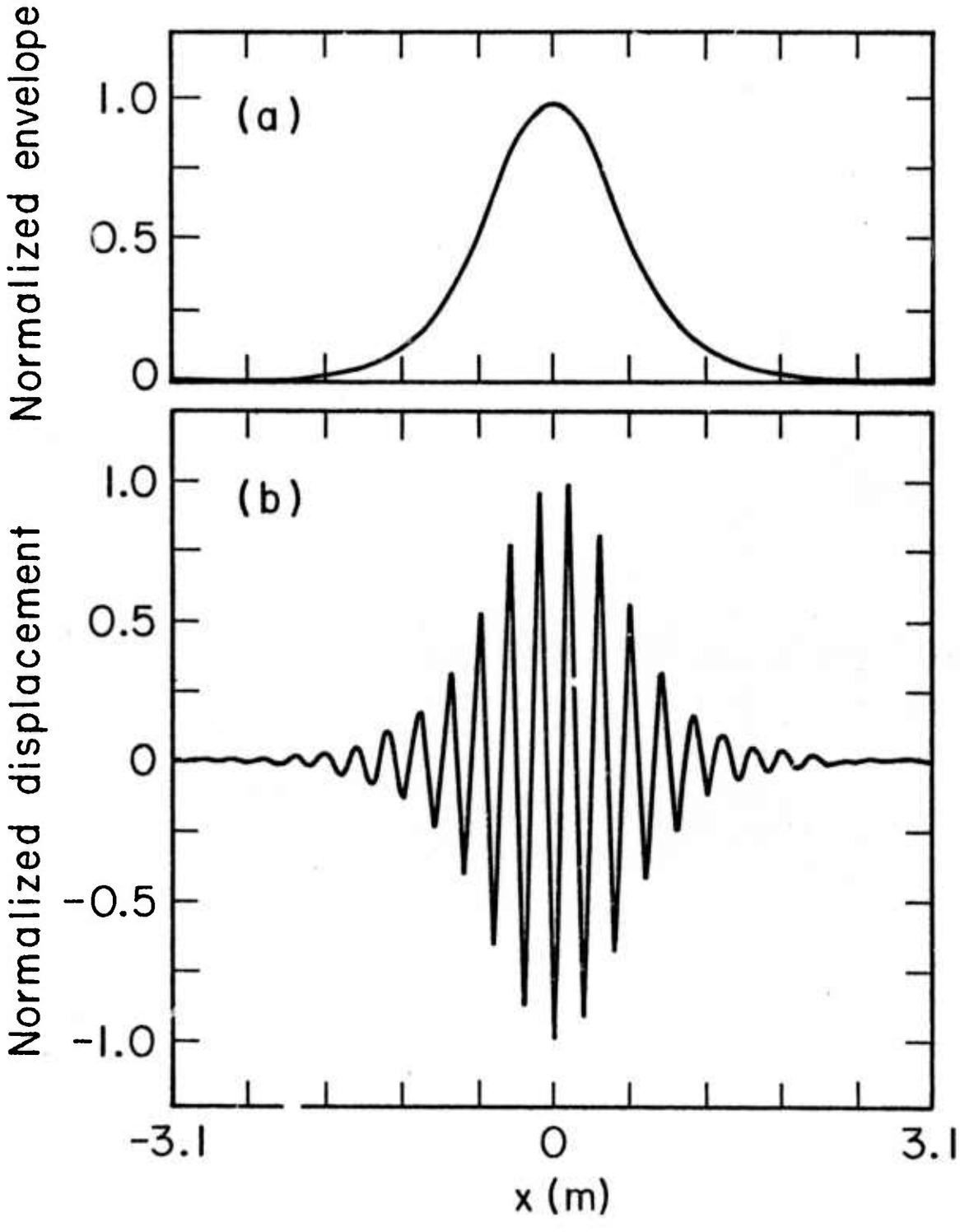

XBL 756-3286

Fig. 2

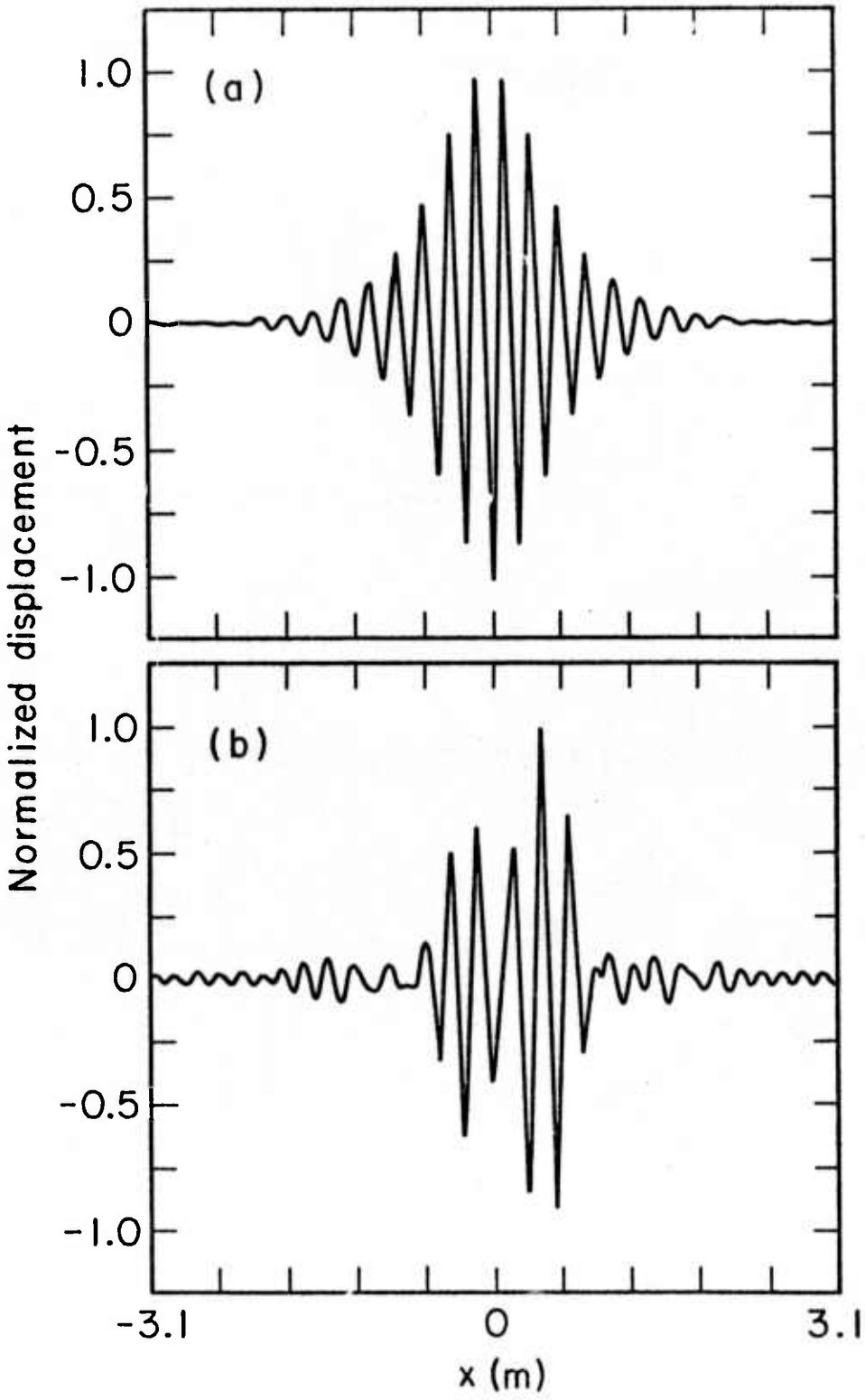

XBL 756-3287

Fig. 3

simply scaled by a factor of four to correspond with the experiment. The viscosity coefficient has been modified in this case to again give the gross attenuation of the pulse. These quantities, along with the slope of the pulse are listed in the second column of Table I.

The initial pulse is depicted in Fig. 3a, as it would be at the wave generator rather than at four feet along the tank as was the soliton in Figs. 1 and 2. This is admittedly not a complete simulation of the experiment. After traveling 28 feet down the tank, however, Fig. 3b shows the same general structure observed for the breakup of the initial waveform.

4. STABILITY*

We discuss first the stability of the soliton solution to Eq. (2.27) given by Eq. (2.41) when a small sinusoidal ripple is impressed on it transverse to the direction of soliton propagation.

Equation (2.27) may be rewritten in a coordinate system translating with a velocity c_g parallel to the x-axis, i.e., $\xi = x - c_g t$, in two dimensions in the more convenient form

$$i \frac{\partial G}{\partial t} = \frac{\omega_K}{8K^2} \left[\frac{\partial^2 G}{\partial \xi^2} - 2 \frac{\partial^2 G}{\partial y^2} + 4K^2 |G|^2 G \right] . \qquad (4.1)$$

From Eq. (4.1) we obtain the relation for the wave energy (in scaled units)

$$i \frac{\partial}{\partial t} |G|^2 = \frac{\omega_K}{8K^2} \left[\frac{\partial}{\partial \xi} \left(G^* \frac{\partial G}{\partial \xi} - G \frac{\partial G^*}{\partial \xi} \right) - 2 \frac{\partial}{\partial y} \left(G^* \frac{\partial G}{\partial y} - G \frac{\partial G^*}{\partial y} \right) \right] . \qquad (4.2)$$

A solution having finite extent in the ξ-direction and periodic boundary conditions in the y-direction then satisfies the energy integral

$$\int_\Sigma |G|^2 \, d\xi \, dy = \text{constant} \qquad (4.3)$$

over the surface area Σ. A developing instability thus extracts energy from the soliton.

*This section is taken largely from Cohen, Watson and West (1975).

The solution of the nonlinear Schrödinger equation which we investigate is of the form

$$G = G_s + Y(\xi,t)\ \cos(\ell y)\ \exp(-i\omega_K m^2 t/4) \qquad (4.4)$$

where G_s represents the soliton solution (2.41) and Y is assumed to be very small relative to the amplitude of the soliton. This is our transverse perturbation. It is convenient to introduce the dimensionless variables

$$\tau \equiv \omega_K t/8$$

$$s \equiv \sqrt{2}\ m\ K\ \xi \qquad (4.5)$$

and to write the perturbation amplitude as the complex function

$$Y(s,t) = U(s,\tau) + i\ V(s,\tau) \quad , \qquad (4.6)$$

where U and V are real. Substituting expression (4.4) into the equation of evolution (4.1), linearizing in Y, and equating to zero the real and imaginary parts of the resulting expression, yields the coupled equations

$$-\frac{\partial V}{\partial \tau} = \frac{\partial^2 U}{\partial s^2} + (H + W)U$$

and

$$\frac{\partial U}{\partial \tau} = \frac{\partial^2 V}{\partial s^2} + (H - W)U \quad . \qquad (4.7)$$

The coefficient functions in Eq. (4.7) are given by

$$H = Q - 1 + 4\ \mathrm{sech}^2(s) \quad ,$$

$$W = 2\ \mathrm{sech}^2(s) \tag{4.8}$$

and

$$Q = \ell^2/(mK)^2 \quad . \tag{4.9}$$

Consider first the case of a simple exponentially growing instability, for which we write

$$U = u(s)\ \exp(E\tau)$$

$$V = v(s)\ \exp(E\tau) \quad .$$

When substituted into Eq. (34) this yields

$$-Ev = u_{ss} + (H + W)u$$

$$Eu = v_{ss} + (H - W)v \quad , \tag{4.10}$$

where the subscript notation for derivatives has been adopted, i.e., $u_s \equiv du/ds$, etc. For stable oscillating perturbations we would, on the other hand, write

$$U = u(s)\ \sin\ (E\tau)$$

$$V = v(s)\ \cos\ (E\tau)$$

which when substituted in Eq. (4.7) yields

$$Ev = u_{ss} + (H + W)u$$

$$Eu = v_{ss} + (H - W)v \quad . \tag{4.11}$$

Since neither set of Eqs. (4.10) and (4.11) is self-adjoint, we have no a priori assurance that normalizable solutions will be found with E real.

At this point it might be observed that our discussion is similar to that of Schmidt (1975) who studied the stability of a plasma wave soliton. His soliton was of the form (2.41), but his equation describing the transverse perturbation was somewhat different from Eqs. (4.7). Schmidt observed that for the case

$$Q = E = 0 \quad ,$$

Eqs. (4.10) and (4.11) have two sets of solutions:

Even Parity: $v = v^{(0)} = \operatorname{sech} s$

$u = 0$

Odd Parity: $v = 0$

$$u = u^{(0)} = dv^{(0)}/ds \quad , \tag{4.12}$$

where the superscript indicates the condition $Q = E = 0$.

The solutions Eqs. (4.12) suggest using perturbation theory to analyze Eqs. (4.10) and (4.11) for small Q, or long wavelength perturbations. Consider first the odd parity case and define the operators

$$\underset{\sim}{L} \equiv (d^2/ds^2) + 2\,\mathrm{sech}^2\, s - 1$$

$$\underset{\sim}{L}' \equiv (d^2/ds^2) + 6\,\mathrm{sech}^2\, s - 1 \quad . \tag{4.13}$$

Equations (4.10) can then be rewritten

$$\underset{\sim}{L}'u = -Ev - Qu$$

$$\underset{\sim}{L}'v = Eu - Qv + 4\,v\,\mathrm{sech}^2\, s \tag{4.14}$$

and using Eq. (4.12),

$$\underset{\sim}{L}'u^{(0)} = 0 \quad . \tag{4.15}$$

Multiplying both expressions in Eqs. (4.14) by $u^{(0)}$ and integrating over all s, using Eqs. (4.15) and substituting the first expression into the second, yields

$$E^2 = -Q^2 + 4Q \int_{-\infty}^{\infty} u^{(0)} v\,\mathrm{sech}^2\, s\, ds \Big/ \int_{-\infty}^{\infty} u^{(0)}\, v\, ds \quad . \tag{4.16}$$

If we write the solution to Eq. (4.14) as a first order correction term,

$$v = E\, v^{(1)} \quad , \tag{4.17}$$

then from the second expression in Eq. (4.14), to lowest order in E and Q, we obtain [see Eqs. (4.13)]

$$\underset{\sim}{L}\, v^{(1)} = u^{(0)} \quad . \tag{4.18}$$

To evaluate the ratio of integrals in Eq. (4.16) and thereby obtain the eigenvalue E, we use the relations

$$\int_{-\infty}^{\infty} u^{(0)} v^{(1)} \operatorname{sech}^2 s \, ds = -\frac{1}{6} = -\frac{1}{4} \int_{-\infty}^{\infty} \left[u^{(0)}\right]^2 ds$$

$$\int_{-\infty}^{\infty} u^{(0)} v^{(1)} ds = -\frac{1}{2} = -\frac{1}{4} \int_{-\infty}^{\infty} \left[v^{(0)}\right]^2 ds \quad .$$

The first of these relations derives directly from Eq. (4.14), whereas the second is the result of a numerical integration. Neglecting Q^2 in Eq. (4.16) we obtain the eigenvalue

$$E \approx 1.16 \, Q^{1/2} \quad . \tag{4.19}$$

Equation (4.18) was numerically evaluated for later use. Also the above integrals were evaluated numerically as a test of the solution.

An analysis similar to the above, starting with the even parity zeroth order solution [see Eqs. (4.12)] gave stable, oscillating modes [the case described by Eqs. (4.11)] for small Q. This contrasts with the results of Schmidt (1975) for plasma waves, where the even parity solution was unstable.

For a shorter wavelength perturbation, corresponding to $Q >> 1$, Eqs. (4.7) have the approximate form

$$-\partial V/\partial \tau = U_{ss} + (Q - 1)U$$

$$\partial U/\partial \tau = V_{ss} + (Q - 1)V \quad . \tag{4.20}$$

These equations describe the propagation of linear waves, decoupled from the soliton. An impressed ripple of short wavelength will thus tend to propagate in accordance with the linear dispersive wave equation.

For $Q > 1$ there is no normalizable solution to Eqs. (4.10) and (4.11) when $E = 0$,* so a transition from simple exponential growth to simple oscillatory behavior is not possible in the range $1 < Q < \infty$.

Equations (4.7) were numerically integrated using the perturbation solution $u = u^{(0)}$, $v = Ev^{(1)}$ as the starting condition for $\tau = 0$. For $Q \leq 1$ simple exponential growth consistent with the result (4.19) seemed to occur (for the two exponentiating periods that the calculation was continued). For $Q = 2$ the U and V solutions oscillated. Growth was not observed within the accuracy of the calculation, but propagation away from the soliton did occur. For $Q = 1.5$ propagation away from the soliton was observed, but at a slower rate. Some growth seemed to occur. The oscillatory motion for the larger Q value is consistent with our conclusions based on Eqs. (4.20).

Defining the e-folding rate γ by the relation $\gamma t = E\tau$,

---

*In this case, Eqs. (4.10) and (4.11) are each equivalent to a one-dimensional Schrodinger equation with an attractive potential. If $Q > 1$, this would correspond to a bound state of positive energy.

we have summarized in Fig. 4 the instability discussed above. The quantity $\gamma\tau_{BF}$ [Eq. (3.14)] is plotted against $Q^{1/2} = \ell/(mK)$. Due to the limited accuracy of our calculations, the growth rate in the interval $Q > 1$ is not shown.

We now discuss the propagation of two specific solitons through a train of waves of wave number significantly different from that of the soliton. For both solitons the interval L was chosen as 100 m, so the wave-number interval was $\Delta k = 0.0628\ m^{-1}$. The starting Fourier amplitudes were obtained using Eq. (3.16). The initial slopes $q_n(0)$ are given in columns (3) and (4) of Table I.

The soliton of column (3) has a central mode number $N = 10$, with amplitudes in the range $6 \leq n \leq 14$. We shall refer to this as the "fat" soliton, since its broad spectrum would seem to violate the conditions under which the nonlinear Schrödinger equation was derived.

Equations (2.5) were integrated for an interval of 20 seconds for the fat soliton with the initial conditions of column (3) in Table I. The wave height ζ, as obtained from Eq. (2.3), is shown in Figs. 5a,b at t = 0 and 50 secs for the fat soliton and in Figs. 6a,b for the "thin" soliton. The corresponding envelope function G for the thin soliton is shown in Figs. 7a,b for t = 0 and 50 secs. Again no distortion is discernable.

We now study the interaction of these two solitons with other wavetrains. For the first case we let the thin

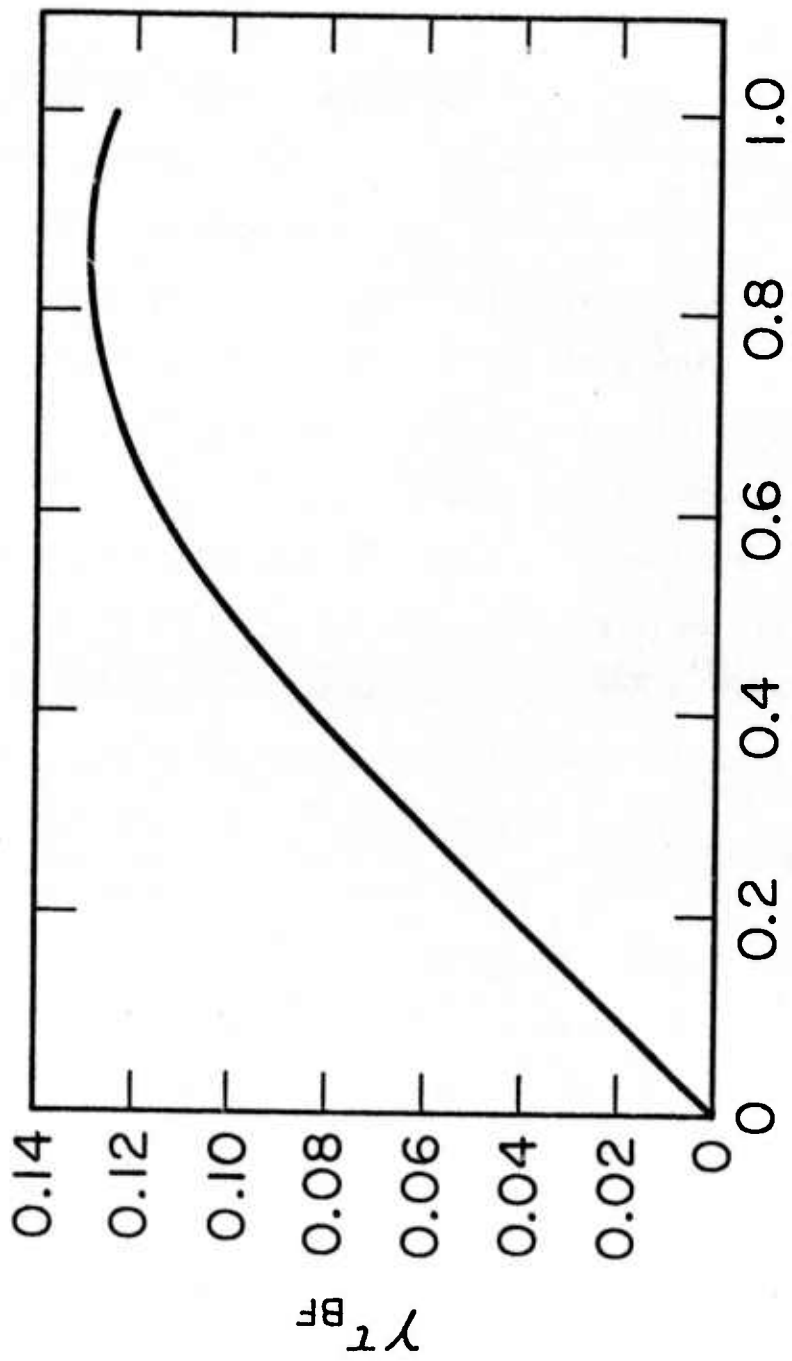

XBL 756-3278

Fig. 4

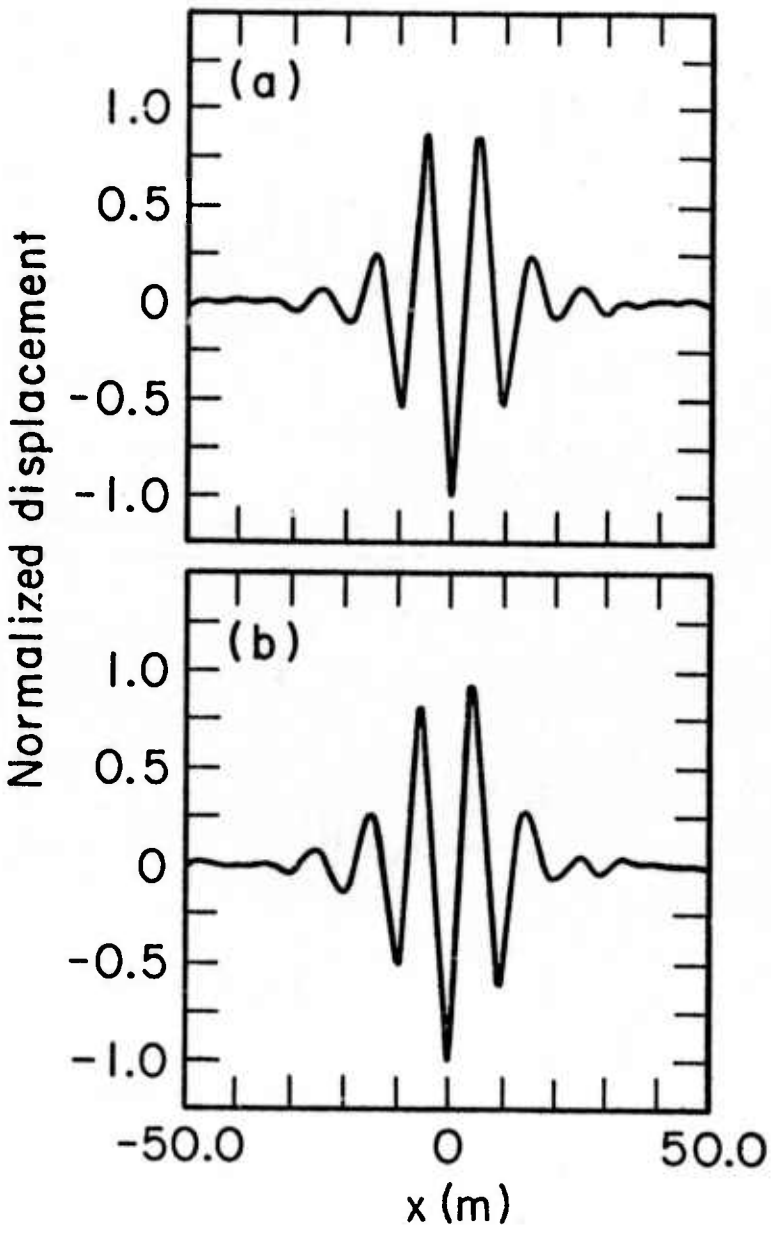

XBL 756-3283

Fig. 5

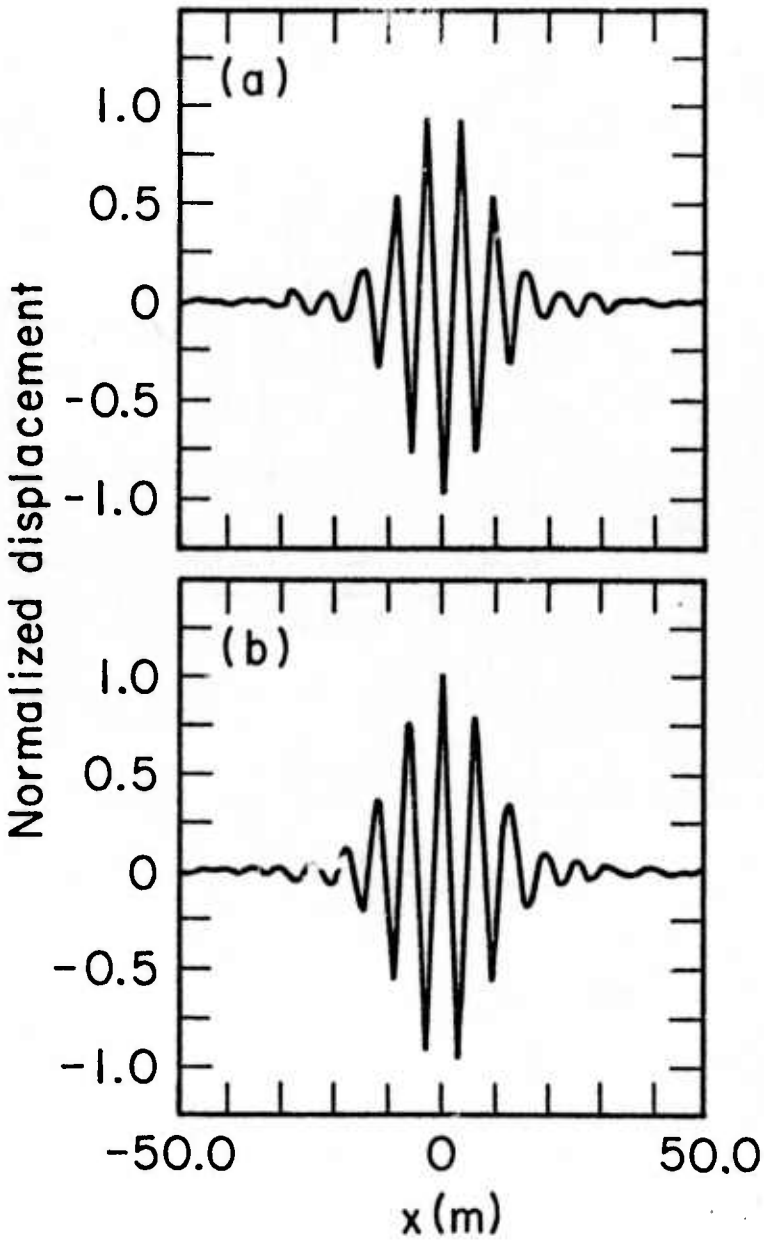
(a)
(b)
1.0
0.5
0
-0.5
-1.0
Normalized displacement
-50.0
0
50.0
x (m)
XBL756-3284

Fig. 6

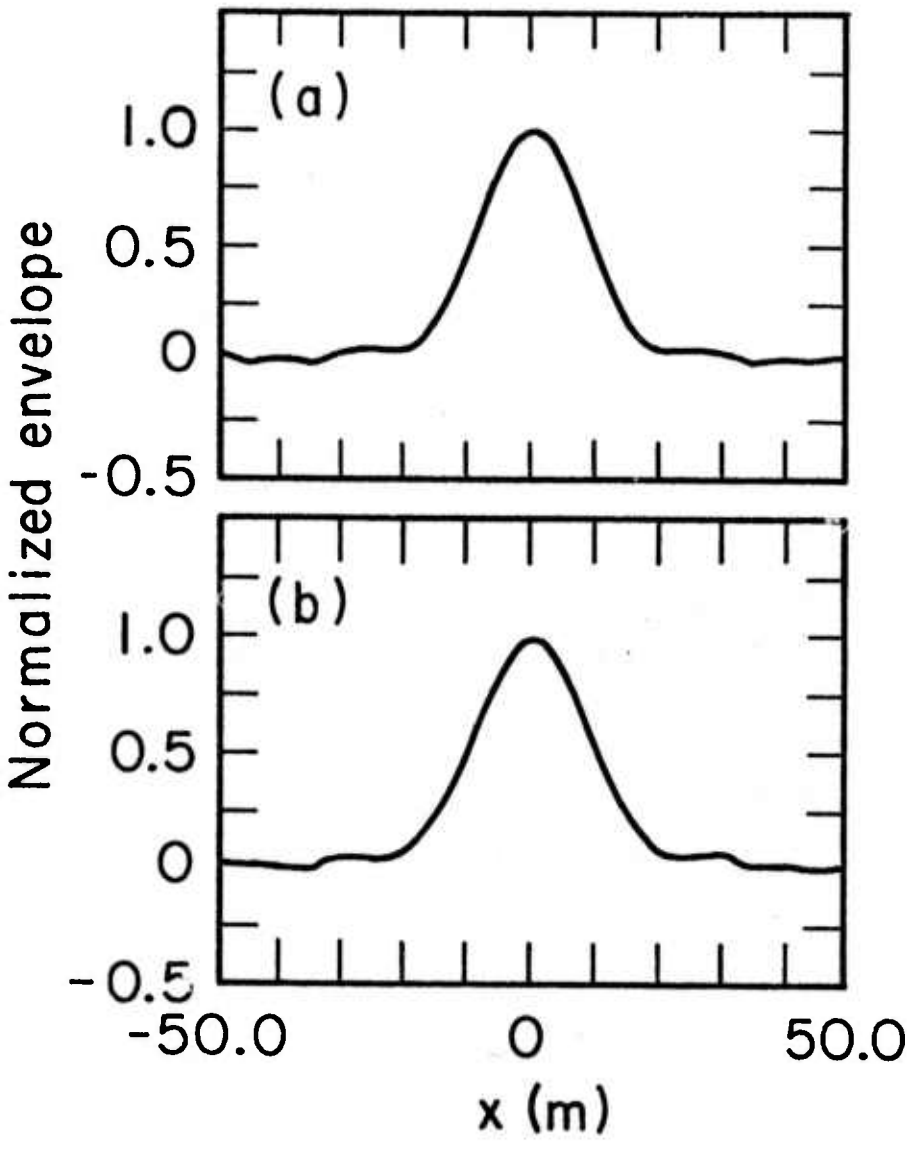

XBL756-3280

Fig. 7

soliton interact with shorter wavelength waves, corresponding to the mode numbers n = 32 and 33. The starting slopes at t = 0 were $q_{32}(0) = 0.1$ and $q_{33}(0) = 0.15$, with respective phases of 0° and 45°. The wave amplitude ζ is shown in Figs. 8a,b,c at t = 0, 30, and 50 seconds, respectively. The envelope function G is shown at these times in Figs. 9a,b,c. Little distortion has occurred at 30 secs. At 50 seconds, however, the soliton edges show an appreciable distortion. It is here where G is small that a modest phase distortion can most readily upset the cancellation of Fourier amplitudes. These results certainly suggest that eventually the soliton would be destroyed by interaction with a spectrum of short wavelength waves.

The next example of soliton interaction involved a train of long wavelength waves, with mode numbers n = 6 and 7. The starting slopes were $q_6(0) = 0.1$ and $q_7(0) = 0.15$, and the thin soliton was again used. The displacement ζ is shown in Figs. 10a-f at various times in the interval $0 \leq t \leq 20$ seconds. Marked distortion occurs at 2 secs, about one wave period at the soliton carrier frequency. The soliton substantially reconvers its shape at 10 seconds and then again at 20 seconds. It would appear that the soliton is being compressed and stretched by the orbital fluid velocity of the interacting wavetrain and that this is to some extent reversible. To investigate this further, the above calculation

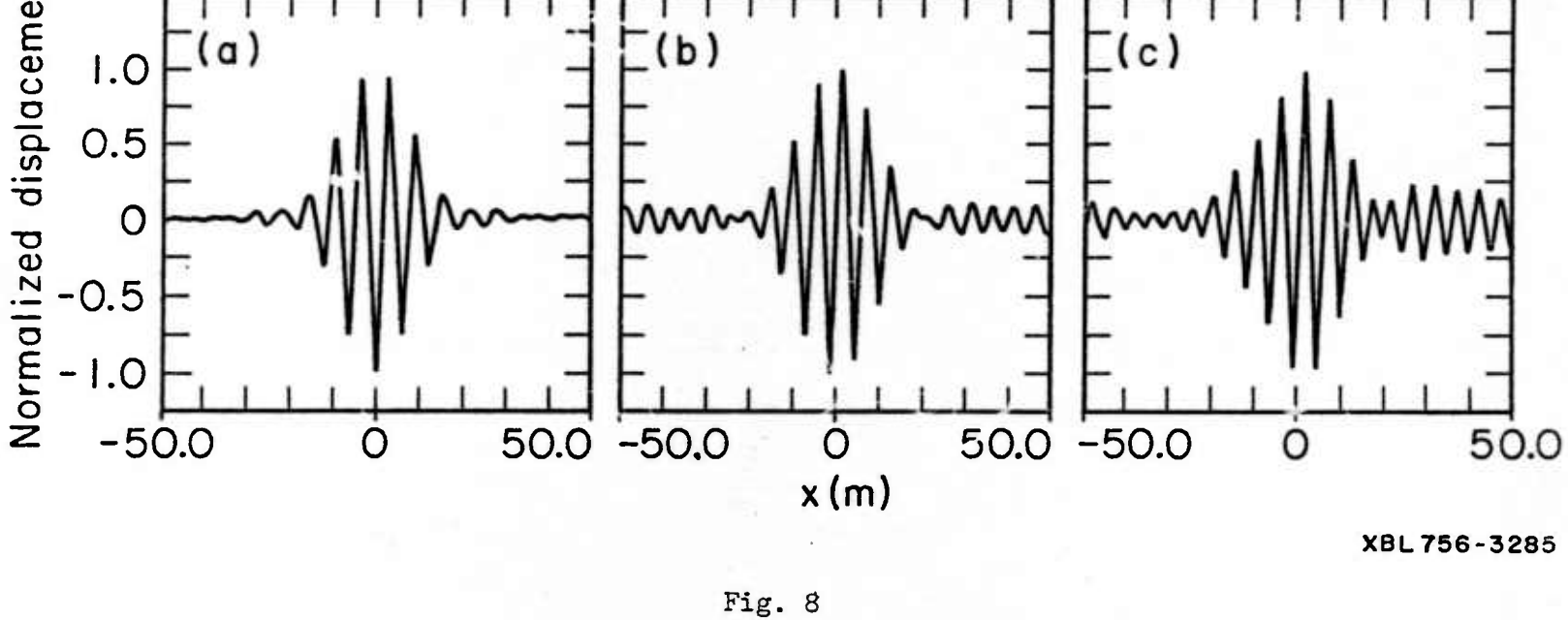

XBL 756-3285

Fig. 8

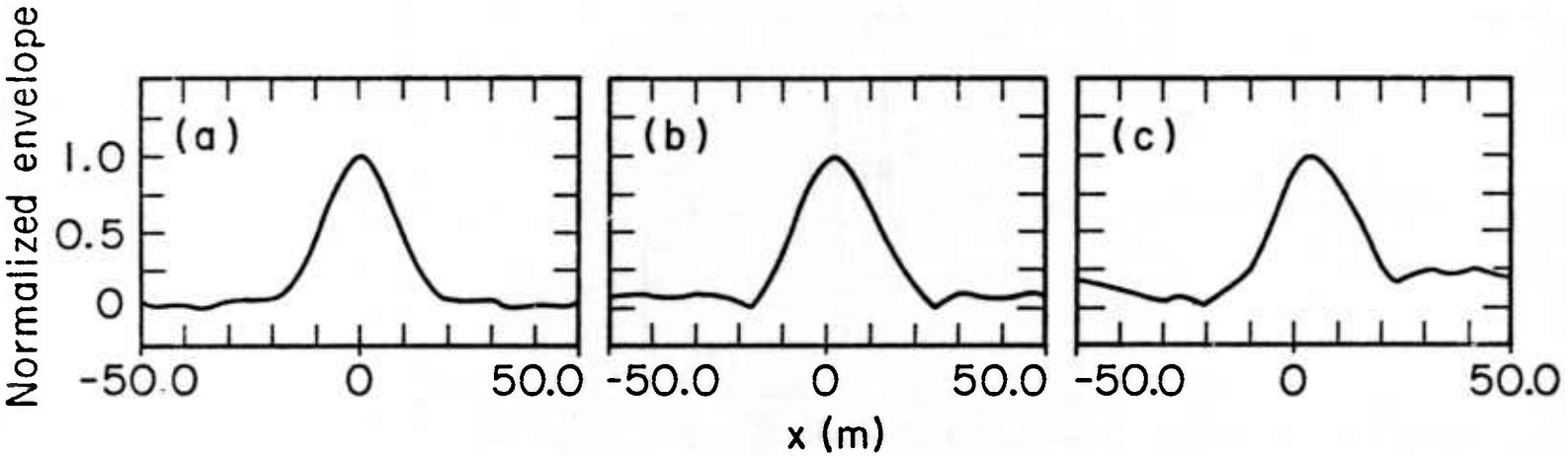

Fig. 9

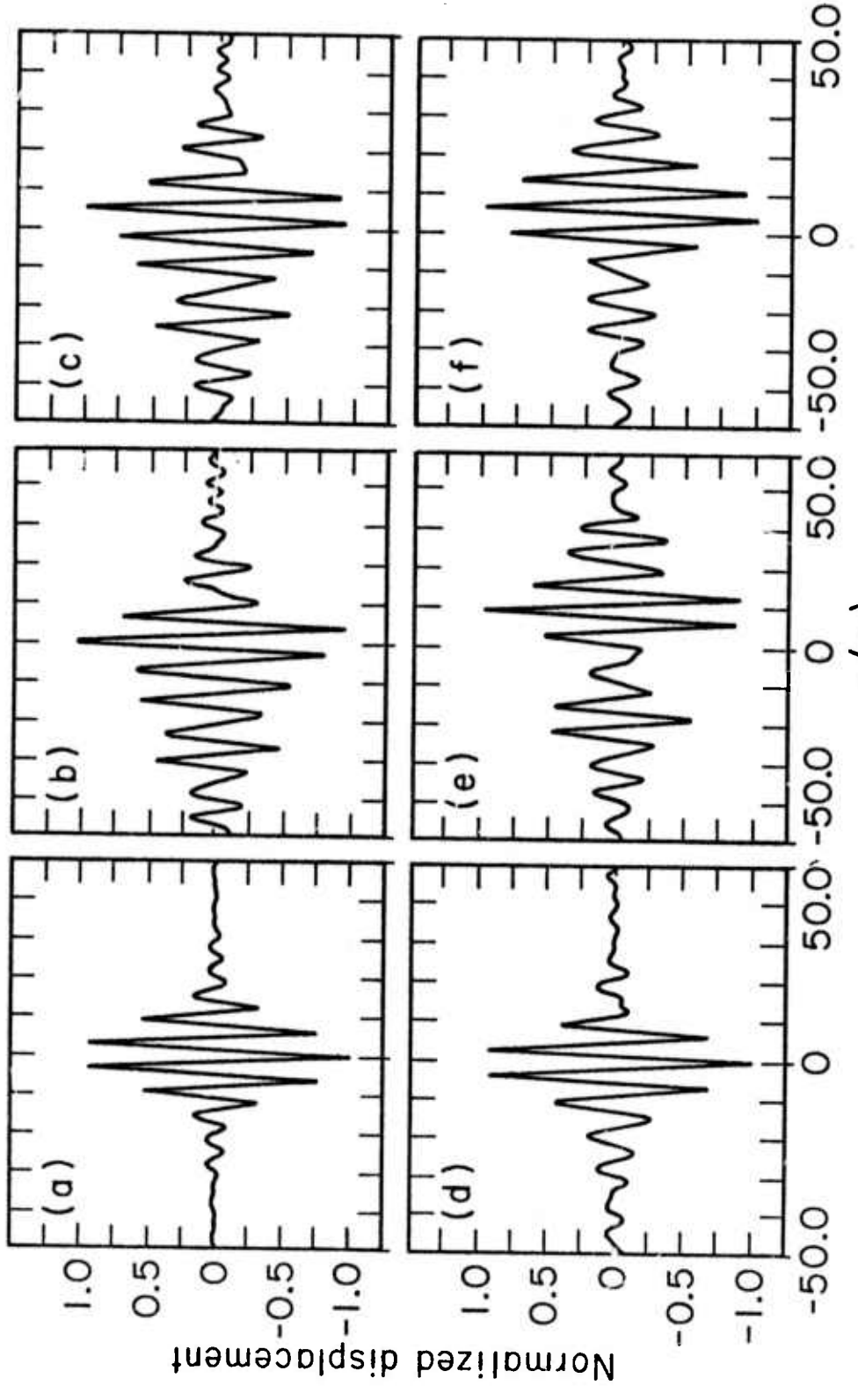

XBL 756-3289

Fig. 10

was repeated but at 10 seconds the amplitudes q_6 and q_7 were set equal to zero. At this time the soliton has the from shown in Fig. 10d. At 20 and 50 seconds it has amplitude shown in Figs. 11a,b. The corresponding envelope function is shown in Figs. 12a,b at 20 and 50 seconds. It is not clear in this time interval that the soliton is undergoing a progressive distortion. The leading edge (to the right) of the envelope function does seem to be steepening somewhat at 50 seconds. A similar asymmetric distortion was noted by Lighthill (1967).

The final illustration studied of soliton interaction was that of the fat soliton interacting with a train of longer waves. These corresponded to modes n = 3 and n = 4, with starting slopes $q_3(0) = 0.06$ and $q_4(0) = 0.09$ and respective phases of 0^c and 45°. The soliton is shown in Figs. 13a-d at times from 0 to 20 seconds. The soliton in this case does not seem to recover, but progressively losses its initial waveform. It should be recalled that this was thought to be a "marginal" soliton.

The above examples suggest that a random field of waves of wavelength much shorter than that of the soliton will probably break up the soliton, but rather slowly. A random wave field of much longer waves can probably destroy a soliton in a few wave periods. A periodic train of long waves distorts the soliton, but it shows some recovery.

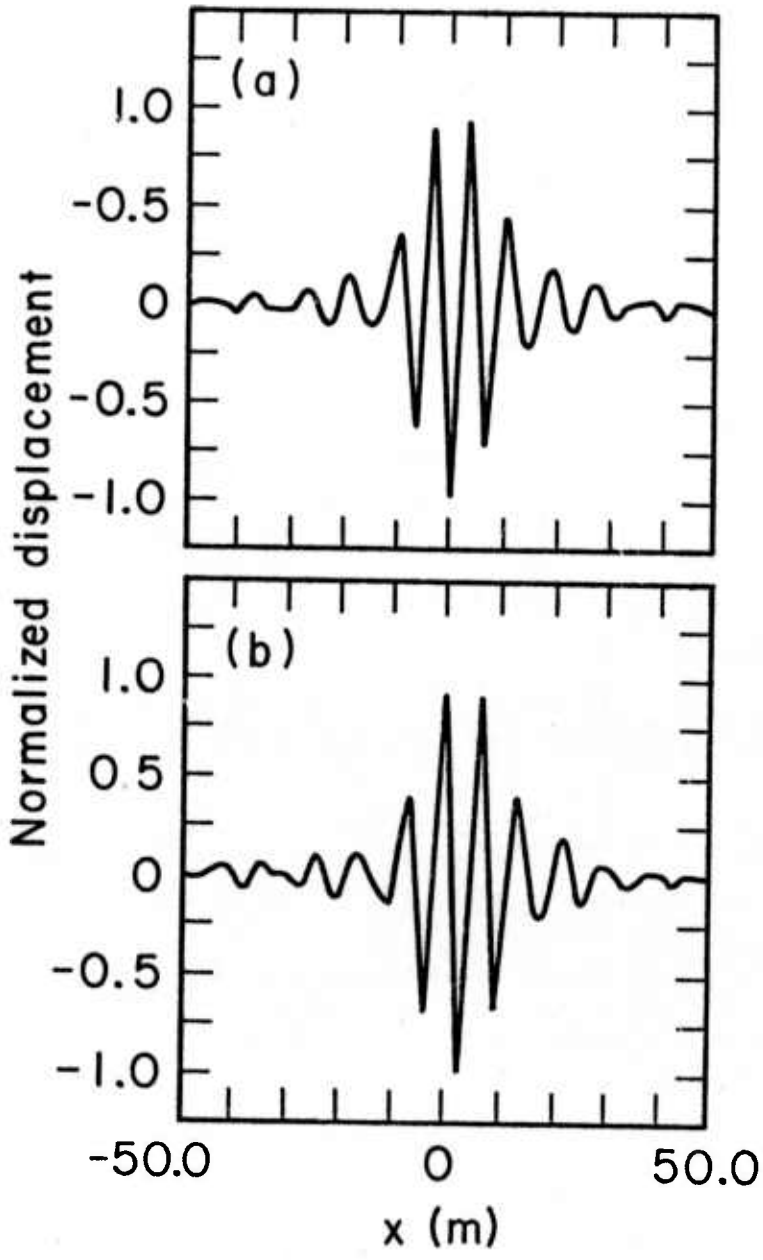

XBL756-3282

Fig. 11

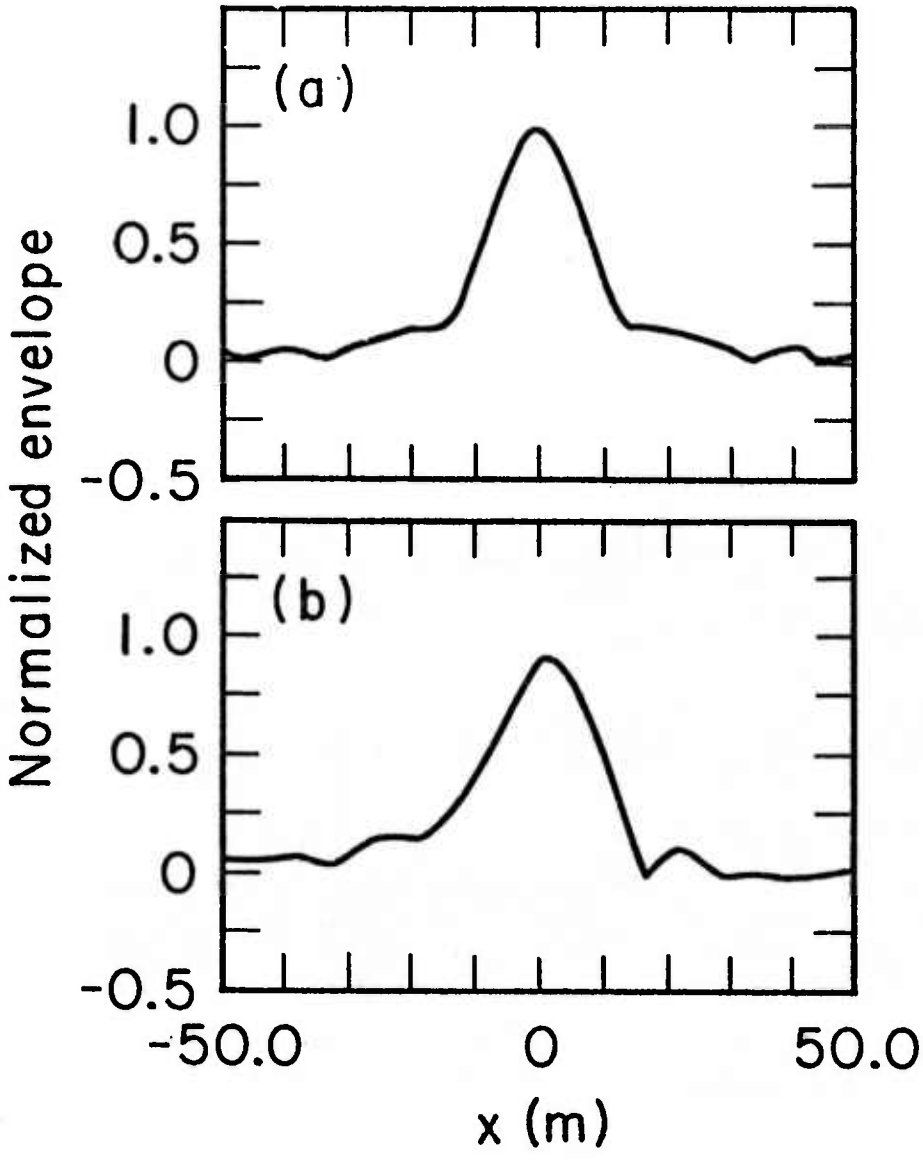

XBL 756-3279

Fig. 12

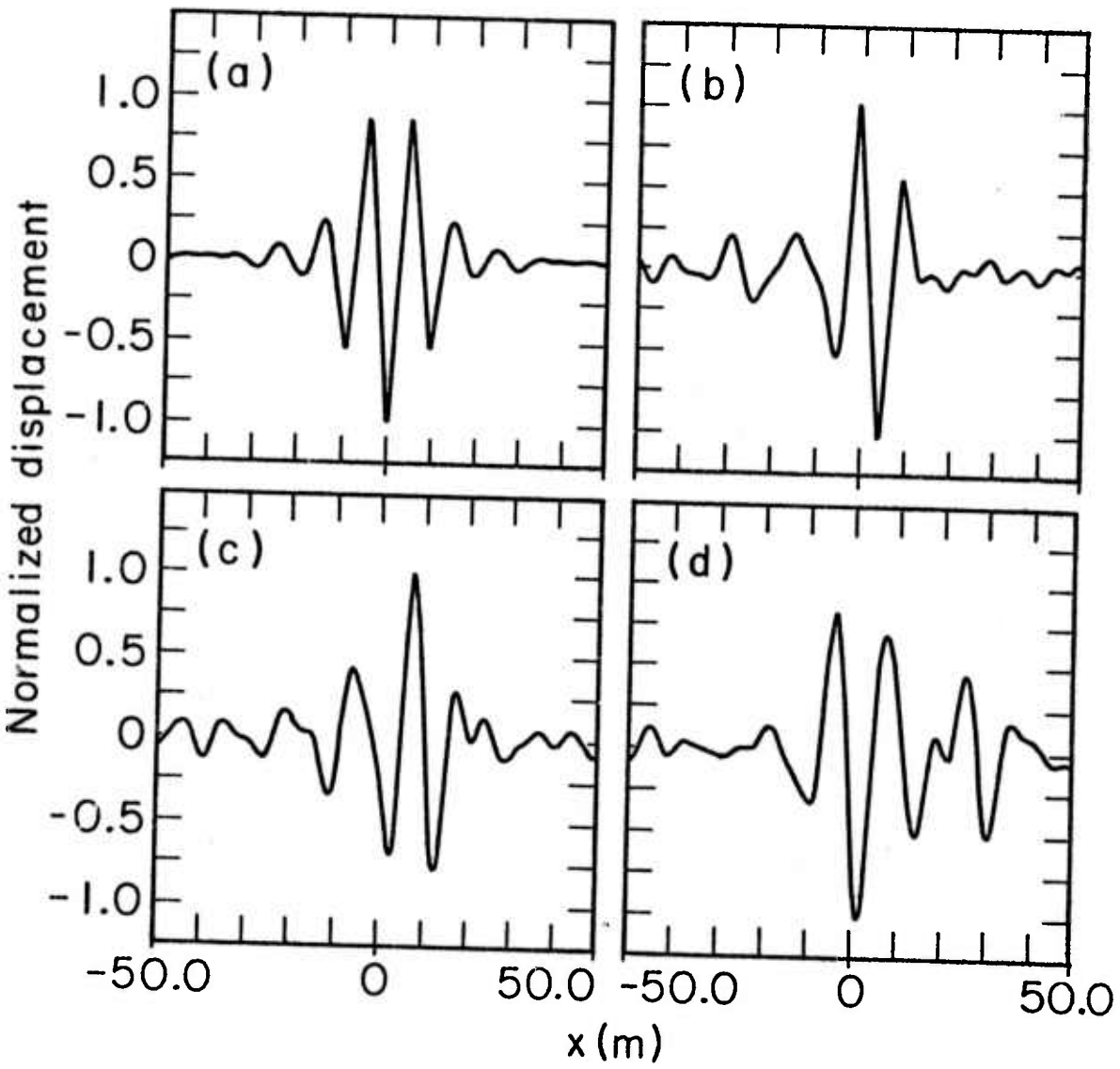

XBL756-3288

Fig. 13

SUMMARY AND CONCLUSIONS

A nonlinear Schrödinger equation is derived from the eigenmode rate equations developed in I, II and III. The solutions to the nonlinear Schrödinger equation are solitons which propagate without change in form as observed experimentally by Feir (1965) and Lake and Yuen (1975).

Although the one dimensional form of the nonlinear Schrödinger equation is the same as that describing the propagation of an electromagnetic pulses in nonlinear optical fibers, the two dimensional equation is different. A linear stability analysis is made for an imposed transverse ripple in this latter equation. A slowly growing instability is found at wavelengths comparable to, or longer than, the length of the soliton. A slowly developing instability is found also for a soliton propagating through a train of waves of wavelength appreciably smaller than that of the soliton. A soliton propagating through a train of waves with wave-length much larger than that of the soliton exhibits gross distortion due to the orbital fluid velocity of the wavetrain. This distortion is to some extent reversible, as the soliton tends to "recover" when the wavetrain is damped to zero amplitude.

The calculations suggest that a random field of waves of wavelengths much shorter than that of the soliton will

probably break up the soliton, but rather slowly. A random wave field of much longer waves can probably destroy the soliton in a few wave periods. A periodic train of long waves distorts the soliton, but it shows some recovery. This suggests that the soliton mechanism will lead to a measurably enhanced correlation times for gravity waves in a random wave field. This speculation can be experimentally tested using a form frequency radar to directly measure the fourth order cumulant of the wave field as discussed in Cohen, Watson and West (1976).

ACKNOWLEDGEMENT

We are indebted to Ralph Janda for doing the calculation depicted in Figure 4. This research was supported by the Defense Advanced Research Projects Agency (DARPA), 1400 Wilson Boulevard, Arlington, VA 22209, and monitored by the Air Force Systems Command, Rome Air Development Center, Griffiss Air Force Base, New York 13440, under Contract F30602-72-C-0494.

FIGURE CAPTIONS

Fig. 1. The soliton specified by the slope amplitudes of column (1), Table I, is shown at t = 0. (a) The envelope G and (b) the wave displacement ζ are normalized to 0.251 cm.

Fig. 2. The soliton of Fig. 1 and its envelope are shown at t = 24 seconds. (a) G and (b) ζ are normalized to 0.115 cm.

Fig. 3. Wave packet with slope amplitudes given in column (2) of Table I is shown in (a) for time t = 0. It is shown at t = 24 seconds in (b).

Fig. 4. The e-folding rate γ for soliton transverse instability is shown in units of the Benjamin-Fier time scale τ_{BF} Eq. (3.14). The quantity Q is defined by Eq. (4.9).

Fig. 5. The "fat" soliton of column (3), Table I, is shown at (a) 0 seconds and (b) 20 seconds. The surface displacement is normalized to 24.7 cm and 23.48 cm, respectively.

Fig. 6. The "thin" soliton of column (4), Table I, is shown at (a) 0 seconds and (b) 50 seconds. The surface displacement is normalized to 10.19 cm and 9.91 cm, respectively.

Fig. 7. The envelope function for the soliton of Fig. 6 is shown at (a) 0 seconds with an A_0 of 10.19 cm

and (b) 50 seconds with an A_0 of 9.91 cm.

Fig. 8. The thin soliton passing through an infinite wavetrain of higher frequency waves is depicted at time t with normalization A_0; (a) t = 0, A_0 = 10.19 cm; (b) t = 30, A_0 = 9.9 cm; (c) 50 seconds, A_0 = 8.4 cm.

Fig. 9. The envelope function for the interacting soliton of Fig. 8 is shown at time t and normalization A_0; (a) t = 0, A_0 = 10.19 cm; (b) t = 30, A_0 = 9.0 cm; (c) 50 seconds, A_0 = 8.4 cm.

Fig. 10. The thin soliton passing through a wavetrain of lower frequency waves is shown at time t and normalization A_0; (a) t = 0, A_0 = 10.19 cm; (b) t = 2, A_0 = 2..27 cm (c) t = 8, A_0 = 20.32 cm; (d) t = 10, A_0 = 16.19 cm; (e) t = 18, A_0 = 17.11 cm; (f) t = 20 seconds, A_0 = 18.22 cm.

Fig. 11. The soliton of Fig. 10 is shown for the case that the interacting wavetrain was damped to zero amplitude at 10 seconds. The times and maximum surface displacements are (a) 20 seconds, 16.42 cm and (b) 50 seconds, 16.11 cm.

Fig. 12. The envelope function, corresponding to the calculation shown in Fig. 11, is shown at time t with corresponding A_0's; (a) 20 seconds, 16.42 cm and (b) 50 seconds, 16.11 cm.

Fig. 13. The fat soliton passing through a lower frequency wavetrain is shown at times t with corresponding

A_0's; (a) 0 seconds, 24.07 cm; (b) 2 seconds, 47.49 cm; (c) 10 seconds, 49.81 cm; (d) 20 seconds and 42.61 cm.

REFERENCES

Benjamin, T.B., J. Fluid Mech. 25 (1966), 241.

Benjamin, T.B. and J.E. Feir, J. Fluid Mech. 27 (1967), 417.

Benney, D.J. and A.C. Newell, J. Math. Phys. 46 (1967), 133.

Case, K.M., K.M. Watson, and B.J. West, Physical Dynamics Report PD-73-047, "Energy Spectra of the Ocean Surface: III. Modulation by a Surface Current," RADC-TR-74-110 (1974).

Chu, V.H. and C.C. Mei, J. Fluid Mech. 41, 1970, 873; ibid. 47, (1971) 337

Cohen, B.I., Watson, K.M., and West, B.J., LBL Preprint (LBL-3266), "Some Properties of Deep Water Solitons" (1975) to appear in Phys. of Fluids (1976)

Davey, A., J. Fluid Mech. 53 (1972), 769.

Diprima, R.C., W. Eckhaus and L.A. Segel, J. Fluid Mech. 49 (1971), 705.

Feir, J.E., Proc. Roy. Soc. A283, (1965) 54

Hammack, J.L. and H. Segur, J. Fluid Mech. 65 (1974) 289.

Hasegawa, A. and F. Tappert, App. Phys. Lett. 23 (1973), 142; ibid. 23 (1973b), 171.

Hasimoto, H. and H. Ono, J. Phys. Soc. of Japan 33 (1972), 805.

Kadomtsev, B.B. and V.I. Karpman, Soviet Phys. Uspelski 14 (1972), 40.

Lake, B.M. and H.C. Yuen, TRW Report (1974), "Nonlinear Deep Water Waves. Theory and Experiment I. Evolution and Interaction of Wave Envelope Pulses." and Phys. Fluids 18 (1975), 956

Lighthill, M.J., J. Inst. Math. Applics 1, 296 (1965); Proc. Roy. Soc. A299, 28 (1967).

Schmidt, G., Phys. Rev. Lett. 34 (1975), 724.

Watanabe, T., J. Phys. Soc. of Japan 27 (1969), 1341.

Watson, K.M., B.J. West, and B.I. Cohen, Physical Dynamics Report PD-73-037, "Energy Spectra of the Ocean Surface: II Interaction with Surface Current," RADC-TR-74-15, (1973)

West, B.J., K.M. Watson, and J.A.L. Thomson, Phys. of Fluids 17, No. 6 (1974), 1059.

Whitham, G.B., J. Fluid Mech 22 (1965), 273.

Whitham, G.B., J. Fluid Mech 27 (1967), 399.

Zakharov, V.E. and A.B. Shabat, Soviet Phys. JETP 34 (1972),62.